Materials Science and Engineering C 41 (2014) 100–118

Contents lists available at ScienceDirect

Materials Science and Engineering C

journal homepage: www.elsevier.com/locate/msec

Review

A review of recent advances in nonenzymatic glucose sensors

Kun Tian, Megan Prestgard, Ashutosh Tiwari *

Nanostructured Materials Research Laboratory, Department of Materials Science and Engineering, University of Utah, Salt Lake City, UT 84112, United States

ARTICLE INFO

Article history:
Received 23 December 2013
Received in revised form 28 February 2014
Accepted 3 April 2014
Available online 13 April 2014

Keywords:
Nonenzymatic glucose sensors
Electrochemical properties
Nanomaterials

ABSTRACT

Currently, there is an overwhelming demand for the development and improvement of glucose sensors. Not only has the number of people requiring these sensors significantly increased over the last decade, so has the demand to make sensors which are both biocompatible and have increased sensing capabilities as compared to current technologies. In order to meet these needs, a move towards nonenzymatic glucose sensors has begun. These new sensors have garnered significant interest due to their capacity to achieve continuous glucose monitoring, their high stability compared to traditional glucose sensors, and the ease of their fabrication. Research has been extensively geared towards the preparation of these nonenzymatic glucose sensors from novel materials, often with unique micro- or nano-structures, which possess ideal properties for electrochemical biosensor applications. In recent years, a variety of materials including noble metals, metal oxides, carbon nanotubes, graphene, polymers, and composites have been explored for their electrocatalytic response to the oxidation of glucose. In this review, the most recent advances in nonenzymatic glucose sensors are visited, with the focus being on the last five years of research.

Contents

1. Introduction

Diabetes mellitus, which is more commonly known as diabetes, has become a universal epidemic. According to the World Health Organization, approximately 350 million people worldwide have diabetes and, based on current projections, diabetes will be the 7th leading cause of death as of 2030 [1,2]. Diabetes is characterized by hyperglycemia, an elevated level of glucose (sugar) in the blood, which can be caused by either inadequate insulin production in the body (Type 1 diabetes) or by the body's inability to use its produced insulin (Type 2 diabetes) [3,4]. Insulin is a hormone that helps the glucose in blood be

* Corresponding author.
E-mail address: tiwari@eng.utah.edu (A. Tiwari).

http://dx.doi.org/10.1016/j.msec.2014.04.013
0928-4931/

absorbed by the body's cells. Both Type 1 and Type 2 diabetes can be treated by externally supplying the necessary insulin to the body; however, if insulin is not given, the glucose levels in the blood can increase to a point where the eyes, kidneys, heart, and nerves may be damaged [4].

Both precise monitoring and careful control of the level of glucose in the blood are essential for the proper diagnosis and treatment of diabetes. Therefore, frequent testing of physiological glucose levels is critical in order to both avoid diabetic emergencies such as hypoglycemia (very low blood sugar levels) as well as to prevent long term complications from arising, which include heart attack, stroke, high blood pressure, kidney failure, blindness, and limb amputation [3,5]. It has been recommended that diabetes patients have their blood glucose levels tested several times a day to ensure they are within the safe range. Thus, for the proper care and management of diabetes, accurate blood glucose level measurement is crucial. These measurements are typically performed using a blood test.

Most of the traditional methods for measuring blood glucose levels employ electrochemical or colorimetric readout systems. Typical glucose level tests, including common handheld glucometers, are done using a small blood sample that is generally obtained through a finger prick. The blood is subsequently introduced to a disposable test strip via capillary action [3]. Most of these tests are based on enzymatic methods, in which the strips consist of either glucose dehydrogenase (GDH) or glucose oxidase (GOx), immobilized on a screen-printed electrode [3,6]. Although this testing enables accurate results, the finger prick method has had poor patient compliance in the past due to the fact that the patient's finger must be pricked using a small pin or lancet to draw blood, which can be quite painful and thus inconvenient for diabetics. In recent decades, various scientific groups have paid considerable attention to the development of more effective and continuous glucose monitoring techniques including invasive and non-invasive monitoring methods using both enzymatic and nonenzymatic sensing techniques. In attempts to improve patient compliance and comfort, recent advances to circumvent the finger prick method have even moved to examining the glucose in tears or the acetone in breath as markers for diabetes [7,8]. These advances stand to make next-generation glucose sensors portable, easy to use, capable of instantaneous readout, lower cost, and pain free. Numerous different methodologies for improving glucose sensor technology have been exploited, including electrochemical monitoring, colorimetric (optical) monitoring, as well as piezoelectric and thermoelectric sensing [3,6,9,10].

The timeline of glucose sensor development can be divided into four primary generations [9–11]. First generation sensors relied on the immobilization of a catalytic enzyme, such as glucose oxidase (GOx), on an electrode. The GOx acts as a catalyst for the reaction of glucose and oxygen, thus glucose is oxidized at the electrode, forming gluconolactone and hydrogen peroxide. Because of this, the concentration of glucose in the initial sample can be determined by detecting the amount of hydrogen peroxide generated at the electrode. However, this reaction requires free oxygen to act as the reaction mediator. This poses a serious problem in the operation of these sensors, as they may not function effectively for oxygen deficient blood samples. A second problem faced by first generation glucose sensors was the interference caused by electroactive species in the blood, such as ascorbic acid, uric acid, and countless other drugs which could be present in the blood [9].

In the second generation of glucose sensor technology, the use of a non-physiological, artificial mediator was proposed to serve as both a replacement to the first generation mediator—oxygen—and as an enhancement for the electron transport process. Thus, the second generation sensors consisted of an immobilized enzymatic catalyst, GOx, on an artificial mediator. Various materials such as ferrocene derivatives and ferricyanide have been used as the artificial mediators [9]. The second generation sensors were able to overcome some of the limitations of the first generation sensors; however, their performance and sensitivity were still dependent on the changes in the pH of the medium and changes in the temperature and humidity of the electrode surface.

In the third generation of glucose sensor technology, efforts were made to eliminate the need for a reaction mediator so as to transfer the electron directly from the enzyme to the electrode. This was done by immobilizing an enzyme to the electrode. Some nano- or microporous materials have been chosen as the substrate for immobilization of the GOx, since the enhanced surface area of electrode surface can increase the electron transfer rate [12]. Though third generation sensors were expected to show some improvement over their first and second generation counterparts, they still suffered from the limitations arising from the dependency of enzyme's activity on the temperature, humidity, interference, etc. Moreover, some additional problems were encountered because the electron transfer process was inhibited by the thick enzyme layer [9,10,13].

The problems associated with these third generation, enzyme based glucose sensors have steered researchers to explore enzyme-free detection. This has led to the development of nonenzymatic glucose (NEG) sensors, which allow glucose to be oxidized directly on the electrode surface. NEG sensors constitute the fourth generation of glucose sensor technology. A tremendous amount of NEG sensor research is going on all around the world, as evidenced by the exponential increase in the number of publications over recent years (see Fig. 1). In this article, we have made an effort to review the most influential and recent advances in NEG sensor technology.

1.1. Electrochemical detection of glucose

Electrochemical sensors are the industry standard for glucose sensing applications because these sensors exhibit quite low detection limits, have enhanced response times, and are of much lower cost compared to the sensors based on other detection mechanisms. Among the electrochemical detection approaches, two specific methods, named potentiometry and amperometry, have been used quite extensively [9]. In potentiometric sensors, potential difference between a reference electrode and a working electrode is measured at zero applied current. The potential of the working electrode changes depending on the glucose concentration. It has been shown that these sensors can measure glucose concentrations of 10 μM or higher (the blood glucose level of a typical human is the range of 4–7 mM) [13]. In amperometric glucose sensors, a constant bias potential is applied and the resulting current, which scales linearly with glucose concentration, is measured. Amperometric sensors have been shown to possess almost similar glucose detection limits as their potentiometric counterparts, typically in the μM to M range [12]. In this review, we have not covered the detailed description of the principle of operation of various NEG sensors, because these details have been covered by another excellent review article published recently by M. Rahman et al. [13].

1.2. Mechanism of glucose oxidation on electrode surface

Electrocatalysts present at the electrode surface are the primary factors affecting the rate of glucose oxidation and hence its detection. In traditional sensors, the enzyme such as GOx is used as a catalyst, while, in NEG sensors, atoms at the surface of the electrode themselves act as the electrocatalysts. Although the mechanism of glucose oxidation at the electrode surface is still not fully understood, there are two main models which have been proposed to explain the above process [11,13,14]. The first model, proposed by Pletcher [15], is known as the activated chemisorption model. It is believed that the oxidation process is initiated through the adsorption of the glucose molecule on the electrode surface. This allows the glucose molecule to form a bond with the electrode surface, where the electrocatalysts aid in the oxidation. At the same time, the hydrogen atom in the glucose molecule, which is attached to the hemiacetal carbon (see Fig. 2), is extracted. Once extracted, this hydrogen atom bonds with the electrode surface at a site

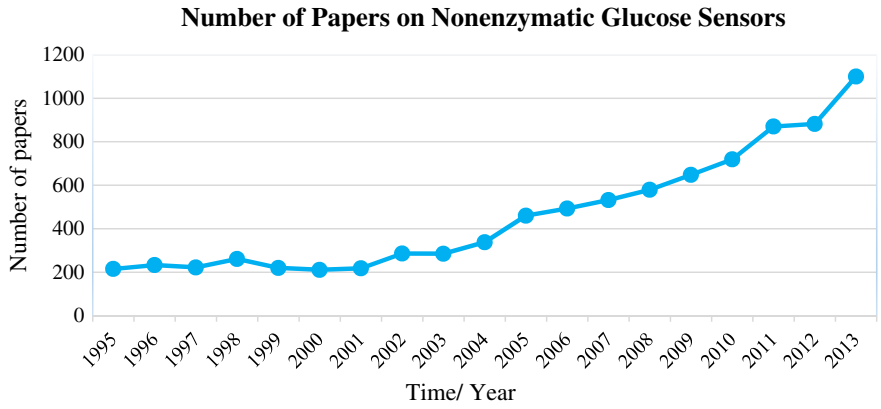

Fig. 1. Number of papers published in the field of NEGs over the last few years (data collected using Google Scholar).

adjacent to the bound glucose [11,13,15]. A change in the oxidation state of the glucose molecule on the metal electrode results in a change in glucose–metal interaction, thereby lowering the glucose–metal bond strength, resulting in desorption of the glucose molecule. Because the electrode surface and the glucose molecules form and break their bonds in the electrocatalytic process, a bond of intermediate strength is desired, as it is conducive for both the adsorption (bond forming) and desorption (bond breaking) processes.

The second model, known as the 'Incipient Hydrous Oxide Adatom Mediator' (IHOAM) model, was proposed by Burke [13,16]. Burke originally formulated this model based on the observation that there are active metal atoms on the electrode surface, which have low lattice stabilization and enhanced reactivity [11,16,17]. These atoms undergo a premonolayer oxidation step, during which an incipient hydrous oxide, OH_{ads}, layer is formed which is believed to mediate the oxidation of glucose at the electrode surface [17]. Fig. 3 shows a schematic illustration of the IHOAM model.

Although both of these models are under scrutiny, they can still be used to explain the oxidation of glucose for different electrode materials.

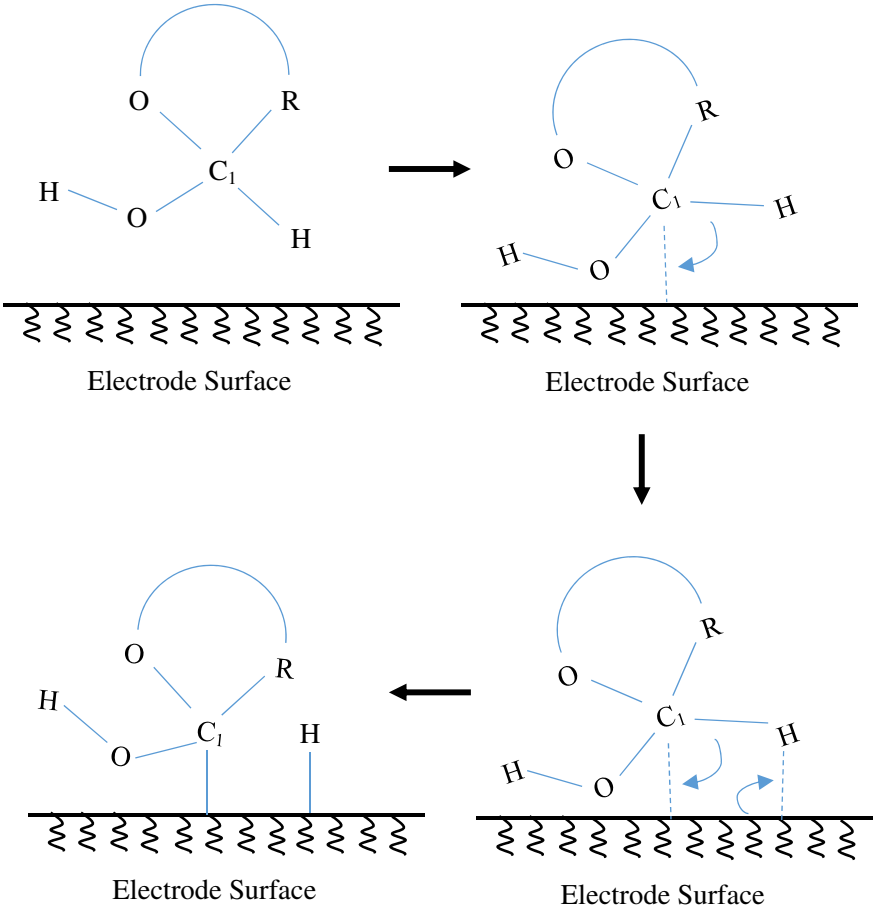

Fig. 2. An illustration of the concentric adsorption theory with adjacent adsorption sites proposed by Pletcher. C_1: hemiacetalic carbon atom. R: the other parts of the glucose molecule.

2. Recent developments in NEG sensors

2.1. Metal and metal compound based glucose sensors

Various metal based electrodes have been studied over the past several decades for application in glucose sensors [9,12]. Throughout these studies it has been shown that the mechanism of direct electro-oxidation of glucose varies significantly depending on the metallic catalyst used in the electrode [10]. Materials used in the most recent years are often not simple metals or metal oxides; rather, most of them are based on composites or hybrids, because of the benefit of their integrated properties and the potential to overcome some of the drawbacks of traditional noble metal electrodes [9,11,12]. The rationale for using these composites originated from the enhanced understanding of the electrocatalytic mechanism of the oxidation of glucose by metals and metal oxides gained in recent years. Thus, in the following part, we will first discuss the electro-oxidation mechanism of glucose in NEG sensors based on different metal and metal oxide systems.

2.1.1. Metal based glucose sensors

In this subsection, we will discuss the oxidation mechanisms, benefits, drawbacks, and recent advances in common metal based (specifically Pt, Au, Ni, Cu, and Ag) glucose sensors.

2.1.1.1. Platinum. In a review by Toghill et al. [10], the cyclic voltammetry (C–V) of a Pt electrode in the presence of glucose has been reported (see Fig. 4). There are three distinct oxidation peaks observed in a typical C–V plot for a Pt electrode at pH of 7. These oxidation peaks correspond to three distinct transformations. The first transformation is the chemisorption and dehydrogenation of the glucose molecule. The second is the dissociation of water to produce hydroxide anions, and the subsequent oxidation of the glucose molecule by the hydroxide ions adsorbed on the surface. And the final transformation is the oxidation of glucose by PtO. Toghill also illustrated the oxidation of glucose as a function of solution pH [10,18]. They found that in acidic solutions, glucose is not very reactive, and the oxidative peaks in the cyclic voltammogram are rather small compared with those appearing in neutral or basic solutions [10,12,18].

Despite the extensive studies on the oxidation process, the use of a Pt electrode for glucose detection has been limited due to the material's many drawbacks [9,10,12]. The first drawback is because the glucose adsorption is highly dependent on the available electrode surface area. The competition of the anions limits the extent of glucose chemisorption and therefore the extent of glucose oxidation. Further, the proportionality of the oxidation current to the concentration of glucose is lost when the electrode surface is saturated. Secondly, Pt electrodes tend to degrade in the presence of species commonly coexisting in physiological solutions, such as amino acids, uric acid, and ascorbic acids as well as chlorine anions and acetaminophen, all of which strongly adhere to the Pt surface, thereby decreasing its electro activity and selectivity.

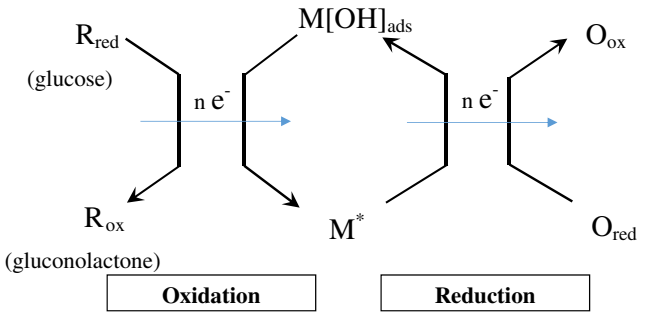

Fig. 3. A schematic illustration of the IHOAM model. M* is the reductive metal adsorption site, and $M[OH]_{ads}$ is the oxidative absorbed hydroxide radical. This figure illustrates how both oxidative and reductive processes are catalyzed at the metal electrode surface.

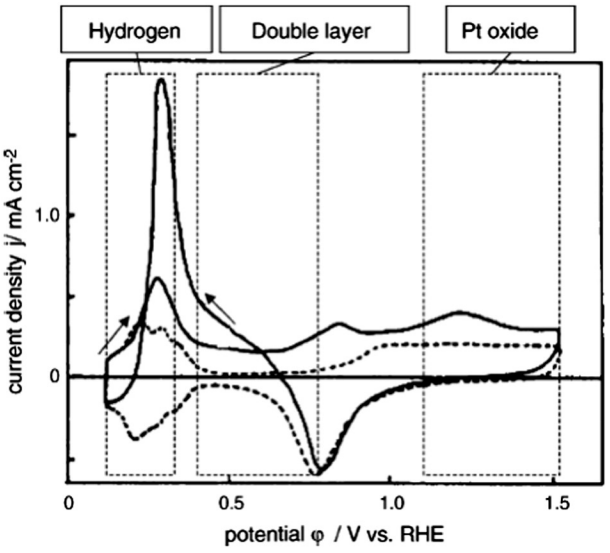

Fig. 4. Cyclic voltammograms in the absence (dotted line) and presence (solid line) of a 0.1 M glucose in phosphate buffer solution at pH 7.5. The graphics display three potential regions where glucose is electrochemically oxidized at a platinum electrode. Reprinted with permission from [12], S. Park, H. Boo and T. D. Chung, Analytica Chimica Acta. 556, 46 (2006). Copyright © 2006, Elsevier.

Third, the cost of Pt is much higher as compared to other materials such as metal oxides and carbon based materials.

Recent studies have explored many ways to overcome the disadvantages of pure Pt electrodes. Pt based alloys have been studied, but their instability and risk of chlorine poisoning have limited their application in glucose detection [19]. Other studies have developed porous Pt structures in order to enhance the amperometric response for NEG sensors, including structures such as mesoporous Pt [20], highly ordered Pt nanotube arrays [21], three-dimensionally macroporous Pt templates [22], and nanoporous Pt electrodes [23]. The motivation for exploring porous structures was based on the fact that highly enlarged electrode areas, especially those of nanoscale texturing can enhance the faradaic currents resulting from the oxidation of glucose. [24,25].

Kim et al. [26] prepared nanoporous Pt films with the roughness factor of 40 by deposition and dealloying of Pt_xSi_{1-x}. The prepared nonenzymatic Pt film sensor exhibited a sensitivity of 10 μA mM^{-1} cm^{-2} and a limit of detection (LOD) of 50 μM in glucose concentrations ranging from 3 to 8 mM [26]. Another way thought to improve the performance of Pt electrodes is to minimize the surface fouling by the use of coating materials such as Nafion (a sulfonated polytetrafluoroethane polymer), polyethylene glycol, and polyurethane, which packages the electrodes [27–29]. For example, Lee et al. [29] designed a NEG sensor based on nanoporous Pt electrode that were fully packaged with a layered biocompatible Nafion and hydrophilic polyurethane membrane. The membrane prevented coexisting protein fouling in biofluidic environments.

2.1.1.2. Gold. It has been reported that Au electrodes can display high electrocatalytic activity toward the oxidation of glucose, and many methods of fabricating Au electrodes have been explored [10]. The earlier studies have shown that the oxidation of glucose by Au electrodes is a multi-step process, and the catalytic component of Au is AuOH, which is formed on the Au surface by the chemisorption of hydroxide anions in elevated pH environments [16,30]. However, Au's chemisorption ability is not as high as that of Pt electrodes [10]. Au electrodes also suffer poisoning by chloride ions in neutral conditions, and by amino acids that fully absorb on the Au surface in both neutral and alkaline conditions, which prevents electro-oxidation completely.

There have been various investigations into the modification of Au electrode materials. Due to the poor chemisorption of glucose on Au electrodes, some have employed mediators in oxidation process of

glucose in order to overcome both the excessive consumption of oxygen as well as to eliminate the interferences in glucose sensors [31], but the sensitivity has still been limited. Another approach is to use ad-atoms (Ag, Hg, Cd, Cu, and platinum group metals such as Ru, Pd, Ir and Pt) or an ad-layer on the Au surface to enhance the electrocatalytic activity [10,12]. More research has been conducted on nanostructured Au materials, based on the idea that small particles not only exhibit greater activity but also that the oxidation mechanism of glucose on Au depends on its surface area and structure [32]. Using nanostructured Au, Aoun et al. [33] found that the electrocatalysis of glucose oxidation is size-dependent.

Kurniawan et al. [34] developed a voltammetric glucose sensor based on Au nanoparticles immobilized on thin Au electrode, grown by a layer-by-layer deposition method. The voltammetric curve of their prepared electrodes is shown in Fig. 5. In the presence of glucose, there are redox peaks clearly visible on the plot. The LOD of the sensor was 0.5 mM and the sensitivity was 160 μA mM^{-1} cm^{-2}, in concentrations of glucose up to 8 mM [34].

2.1.1.3. Nickel. Researchers believe that Ni (II) and Ni (III) couple on the nickel anode surface during the electro-oxidation of glucose in an alkaline environment. First, the $Ni(OH)_2$ is oxidized to the catalytically active NiOOH. Second, the glucose undergoes hydrogen abstraction at the surface to form a radical intermediate and reform the $Ni(OH)_2$ species. Finally, the hydroxyl anions in the solution rapidly oxidize the organic radical intermediate to form gluconolactone [10]. Unlike Au and Pt, the surface of the Ni is immediately oxidized to an oxyhydroxide state at a certain potential, rather than forming a hydrous premonolayer. In addition, the cyclic voltammetry plots of glucose oxidation on a Ni electrode showed no fouling by adsorbed interference species [10]. The disadvantage of Ni electrodes mainly comes from their inability to electrocatalyze in low or neutral pH solutions, since the NiOOH catalysis is dependent on the hydroxyl anions [10]. Another problem is in the competitive interference of ethanol, which affects the blood glucose detection.

To solve these drawbacks of plain Ni electrodes, Ni nanostructured materials with high surface areas have been explored. In a recent study, a nanoflower α-$Ni(OH)_2$-based NEG sensor was prepared by

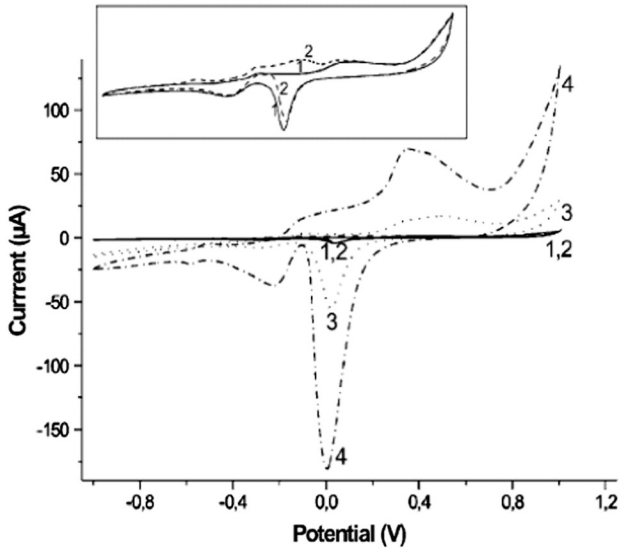

Fig. 5. Voltammograms of uncoated gold electrodes (curves 1, 3) and gold electrodes coated by a layer consisting of polyacrylic acid and gold nanoparticles (curves 2, 4) in 0.1 M NaOH in the absence (curves 1, 2) and the presence (curves 3, 4) of 0.5 mM glucose. Sweep rate: 20 mV/s. Inset: curves 1 and 2 with magnification of the current scale. Reprinted with permission from [34], F. Kurniawan, V. Tsakova and V. M. Mirsky, Electroanalysis. **18**, 1937 (2006). Copyright © 2006 WILEY-VCH Verlag GmbH & Co. KGaA, Weinheim.

Tong et al. [35] using a homogeneous coordination precipitation approach in the $Ni(NO_3)^{2+}$ urea system. They used X-ray diffraction (XRD), Field-Emission Scanning Electron Microscopy (FE-SEM), and Transmission Electron Microscopy (TEM) to verify the morphology and the phase conversion of the complex α- and β-$Ni(OH)_2$ architectures. It was also confirmed that the nanoflower α-$Ni(OH)_2$ has improved glucose sensing performance as compared to traditional Ni.

In another study, 3-D porous nanostructured Ni was fabricated by Niu et al. [36] in which Ni networks were grown on a screen-printed carbon electrode substrate via electrochemically reducing precursors with continuously liberating hydrogen bubbles. Due to the increase in active surface area, the as-prepared glucose sensor exhibited enhanced performance in the linear detection range from 0.5 μM to 4 mM, with an LOD of 0.07 μM, and the sensitivity of 2.9 mA mM^{-1} cm^{-2} [36].

2.1.1.4. Copper. Similar to Ni, the electrocatalysis for the oxidation of glucose in copper based systems is mediated by the redox couple of Cu (II) and Cu (III). Cu is of relatively lower cost as compared to Au or Pt, thus considerable attention has been paid to Cu based NEG sensors in the last few years. Zhang et al. [37] developed one-dimensional Cu nanowires (Cu NWs) by a wet-chemistry method, which had an aspect ratio over 200 and an average length of 30 μm. Specifically, they used the glassy carbon electrodes (GCEs) as electrode substrate. GCEs are very versatile as they provide high sensitivity, negligible porosity, good mechanical rigidity, and they can be altered by means of various modifiers such as Nafion, chitosan, and metal nanomaterials [38–42]. In this study, they prepared glucose sensors containing Nafion/Cu NWs/GCE, which exhibited a sensitivity of 420.3 μA mM^{-1} cm^{-2} and an LOD of 35 nM [37], with interferences at the physiological concentration level being insignificant. Other electrode substrates, especially conductive oxide coated glasses are also commonly used in development of NEG sensors, such as tin-doped indium oxide (ITO), fluorine-doped tin oxide (FTO), etc. Niu et al. [42] prepared a NEG sensor based on a Cu foam structure, with a uniform porosity of 100 μm. They showed that the Cu foam offered promise for glucose detection because of its large surface area enhancement and large pore volume. The Cu foam based NEG sensor showed a linear detection range of glucose concentrations up to 5 mM with a sensitivity of 1810 μA mM^{-1} cm^{-2} and an LOD of 0.98 μM [42]. However, the overall weakness of the distinct redox couple in the Cu system has limited its use and thus CuO has been more commonly explored [13].

2.1.1.5. Other metals. Most of the other noble metals except for Pt and Au have not been investigated due to their relatively weak electrocatalytic activity. However, Ag and Pd have shown some electrocatalytic sensing capabilities. Porous tubular nanostructured palladium-based NEG sensors have been proposed by Bai et al. [43], which were fabricated by electrodeposition of Pd into a CdS modified alumina template, after which the template was removed. Xianyu et al. [44] reported a Ag-based NEG sensor using colorimetric detection. With negatively charged Au nanorods (Au NRs) acting as substrate, the Ag^+ ions in the solution concentrate around Au NRs and serve as the catalyst to react with the glucose. The reaction produces Ag nanoparticles (Ag NPs) that show a light yellow color. The concentration of the Ag NPs correlates directly to the concentration of glucose and was detected by the color change using ultraviolet–visible spectrophotometry (UV–vis) spectrometer.

2.1.2. Metal compound based glucose sensors

During the last few years, several groups have explored different metal oxides for application in NEG sensors [9,11,13]. Metal oxides possess excellent properties for electrochemical biosensors, namely, controllable size, functional biocompatibility, chemical stability, catalytic activity, enhanced electron-transfer kinetics, strong adsorption capabilities, and the capacity to be modified using various other materials [13]. Using state-of-the-art nanofabrication techniques, metal oxides with various morphologies and structures have been exploited [9,11]. Herein,

the most recent advances on metal compound based NEG sensors will be presented.

2.1.2.1. Copper compounds. Copper oxide is a promising material for making NEG sensors because it shows high electrochemical activity, is low cost, is non-toxic, and can be readily modified with other materials [45,48]. The oxidation mechanism of glucose on modified CuO-based electrodes in alkaline solution is believed to be assisted by the redox couple of Cu (II) and Cu (III) [46]. Specifically, the nonenzymatic electro-oxidation process of glucose on CuO surface in an alkaline medium proceeds as follows [47]:

$$CuO + OH^- \rightarrow CuOOH + e^- \quad (1)$$

$$CuOOH + e^- + \text{glucose} \rightarrow CuO + OH^- + \text{glucose acid} \quad (2)$$

Lots of work is going on in this field to develop new and novel techniques to fabricate CuO nanostructures. Cao et al. [45] reported the fabrication of CuO microfibers embedded with CuO nanoparticles, by using a combination of electrospinning and calcination techniques. Their method involves dissolving precursory $Cu(NO_3)_2$ in polyvinyl alcohol (PVA) and electrospinning the subsequent solution on an FTO substrate, after which the PVA was removed by heat treatment. Using the same method, Liu et al. [46] prepared CuO nanofibers with $Cu(NO_3)_2$ and polyvinylpyrrolidone (PVP) as precursors.

Huang et al. [47] prepared CuO nanoparticles by a hydrothermal method using a $Cu(CH_3COO)_2$ precursor. Ibupoto et al. [48] fabricated CuO nanosheets using $Cu(CH_3COO)_2 \cdot 2.5H_2O$ and hexamethylenetetramine precursors. Reitz et al. [49] prepared CuO nano-sphere based NEG sensors by the same method, with $Cu(CH_3COO)_2$ as the precursor. Sun et al. [50] prepared CuO nanoflowers by an in-situ dissolution–precipitation formation mechanism using a one-pot water/ethanol solution-phase transformation of $Cu_2(NO_3)(OH)_3$. They demonstrated that morphology-controlled growth of the nanostructured CuO can be achieved by changing the volumetric ratio of water and ethanol. Using a different precursor of $Cu_7C_{l4}(OH)_{10}H_2O$, Sun et al. [51] obtained CuO nanourchins. To prepare hierarchical nanostructured CuO, a combination of homogeneous precipitation and a microwave-assisted method was introduced by Meher et al. [52]. The resulting structure was CuO nanocrystals sandwiched between microsheet copper oxide layers. The SEM and TEM images of various nanostructured CuO samples referenced above are shown in Fig. 6.

In Table 1, recent publications on various nanostructured CuO based NEG sensors are listed, with details given on their sensitivity, detection limit, detection range, applied potential, and publication year. Further advances have been made towards the integration of nanostructured CuO with carbon nanotubes (CNTs) and graphene, in order to amplify the electroactive surface as well as electrical conductivity for the electro-oxidation of glucose [9]. The use of CNTs and graphene in glucose biosensor materials will be illustrated in Sections 2.2.1 and 2.2.2.

As mentioned previously, Cu metal-based compounds have likewise gained interest for fabricating NEG sensors. Specifically, there are numerous studies on CuS-modified electrode materials for NEG sensors. Lin et al. [53] prepared CuS nanotubes via a microwave transformation and crystallization process with the assistance of diethanolamine. The synthesized CuS nanotubes had porous exteriors, hollow interiors, and rectangular cross-sections that gave the nanotubes particularly high specific surface areas. Liu et al. [54] have shown that the use of solvothermal synthesis can lead to the preparation of sphere-like CuS microcrystals with diameters of approximately 3–5 μm. These CuS nanotube-modified electrodes showed potential application in glucose detection, but the sensitivity, detection range and other performance factors were poor as compared to CuO.

2.1.2.2. Other metal compounds. Several other metal oxides have been exploited for improved electrochemical properties in NEG sensors. Recent publications on this have been collected, and their performance in glucose detection is summarized in Table 2, for materials including nickel oxides, iron oxides, cobalt oxides, silver oxides, and ruthenium oxides.

NiO materials have been commonly employed for their electrocatalytic properties. For application in electrochemical glucose sensors, the oxidation mechanism is attributed to the redox couple of Ni (II) and Ni (III) similar to that of CuO. The nonenzymatic electro-oxidation of glucose on a NiO coated electrode in a basic environment is shown in the equation below [55]:

$$NiO + OH^- \rightarrow NiO(OH) + e^- \quad (3)$$

Using an electrodeposition method, a three-dimensional NiO foam structure was fabricated by Guo et al. [55]. Cao et al. [56] fabricated another unique NiO-based electrode; NiO microfibers on an FTO substrate, fabricated by electrospinning and calcination.

Other materials investigated included iron oxides. Cao et al. [57] obtained FeOOH nanowire-modified electrodes by a wet chemical approach, which showed potential in glucose sensing, but were limited by lack of sensitivity. The oxidation mechanism for these iron oxides can be explained by the redox couple of Fe (II) and Fe (III), similar to the previous two cases, Ni and Cu. A second nanostructure of Fe_2O_3 studied was nanowire arrays by the same authors [58] in 2011, made using the same general processing, but which showed higher detection performance.

Various forms of cobalt oxide have likewise been studied. Kung et al. [59] prepared acicular cobalt oxide nanorods (CoO NRs) on FTO via a chemical bath deposition technique followed by annealing. Via TEM, SEM and XRD, they found the prepared films were composed of layered cobalt carbonate hydroxide (LCCH) when annealed at 200 °C and at and above 300 °C the LCCH was converted to a CoO NRs film, which was composed of tiny Co_3O_4 nanoparticles. Due to the redox couple of Co (III) and Co (IV), which can easily oxidize glucose to gluconolactone, Co_3O_4 nanoparticles (Co_3O_4 NPs) were fabricated by Hou et al. [60] using a metal-organic framework (MOF), zeolithic imidazolic-8, as template. The results of both the CoO NRs film and Co_3O_4 NPs electrodes showed promise in the application of glucose detection. In the final system discussed, combinative ruthenium oxide (RuO_x) and Prussian blue (MCN, PB) analogues, (designated as $mvRuO_x$–MCN, mv: mixed valence, M: Fe, Ru) were fabricated to mediate glucose oxidation [61]. Used in conjunction with a modified screen printed electrode (SPE), Kumar et al. [61] showed the oxidation of glucose in the $mvRuO_x$–RuCN/SPE system in acidic solution was comparable to a classic RuO_2 electrode in an alkaline environment, which is due to the mediation of the high oxy/hydroxyl-Ru (VII) and Ru (VI) redox states.

2.2. Composite based glucose sensors

Composite NEG sensors have drawn a lot of interest for the integration of advantageous properties from many different materials, such as the large electrical conductivity of metals, the selectivity of organic materials, and the electrocatalytic activity of metal oxides [11–13]. In the following subsections, alloys, metals and metal oxide composites, and polymer modified composites are discussed, focusing on the most advanced research on NEG sensors. We further emphasize the motivation of composite glucose sensors, their application for glucose detection, and the various fabrication methods.

2.2.1. Alloys or bimetallic composite based glucose sensors

In recent studies, the use of alloys and bi-metals as electrode materials has been explored in order to develop synergetic and effective electrocatalysts, see Table 3. Electrodes have been commonly based on the combinations of metals such as Pt, Pb, Au, Ag, Pd, Rh, Co, Cu, and Ni [19,62–68].

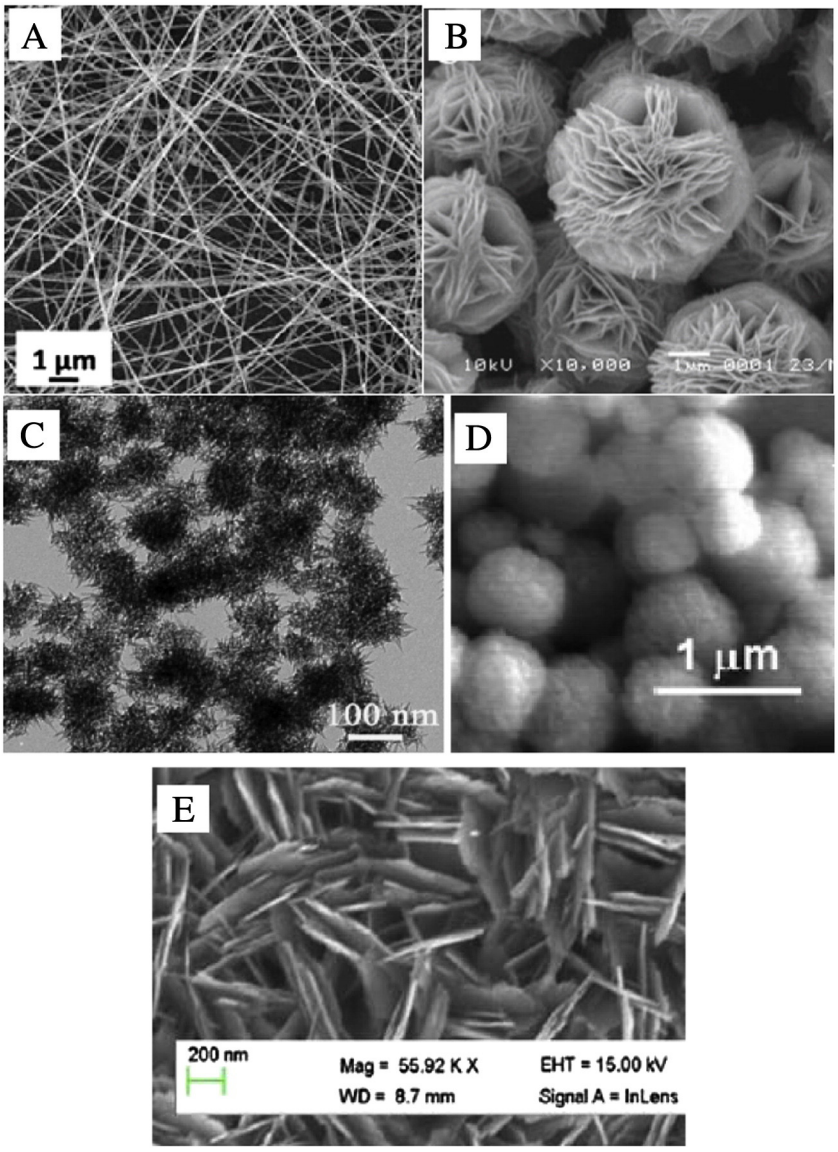

Fig. 6. SEM and TEM images of different nanostructured copper compounds. (A) CuO nanofibers (SEM). Reprinted with permission from [46], G. Liu, B. Zheng, Y. Jiang, Y. Cai, J. Dua, H. Yuan, D. Xiao, Talanta. **101**, 24 (2012). © 2012, Elsevier; (B) Sphere-like CuS microcrystals (SEM). Reprinted with permission from [53], J. Lin, F. Tao, L. Wang, J. Mater. Sci. **48**, 5509 (2013). © Springer; (C) CuO nanourchins (TEM). Reprinted with permission from [51], S. Sun, X. Zhang, Y. Sun, S. Yang, X. Song and Z. Yang, ACS Appl. Mater. Interfaces. **5**, 4429 (2013). © 2013, American Chemical Society; (D) CuO nanospheres (SEM). Reprinted with permission from [49], E. Reitz, W. Jia, M. Gentile, Y. Wang, Y. Lei, Electroanalysis. **22**, 2482 (2008). © 2008 WILEY-VCH Verlag GmbH & Co. KGaA, Weinheim; (E) CuO nanosheets (SEM). Reprinted with permission from [48], Z. H. Ibupoto, K. Khun, V. Beni, X. Liu and M. Willander, Sensors. **13**, 7926 (2013). © MDPI OPEM ACCESS.

In a study conducted by Sun et al. [69], electrode arrays were prepared containing combinations of Pt, Pb, Au, Pd, and Rh, and tested for their amperometric response. These results established that the binary, ternary, and higher Pt/Pb alloy composites were the most active electrocatalysts. In addition, the Pt/Pb alloy composites catalyzed the oxidation of glucose at more negative potentials than those for pure Pt in nonenzymatic voltammetric measurements, which enabled the Pt/Pb alloys to be more resistive to interfering agents (ascorbic and uric acids and 4-acetamidophenol) as these are oxidized at more positive potentials. However, the performance of these Pt/Pb alloy catalysts

Table 1
Nanostructured CuO based NEGs and their detection performance. Measurements were performed using amperometric technique.

Electrode matrix	Sensitivity/μA mM^{-1} cm^{-2}	LOD	Linear range	Applied potential/V	Publication year and reference
CuO microfibers/CuO nanoparticles/FTO	2321	2.2 nM	Up to 0.6 mM	0.40	2012, [45]
CuO nanofibers/ITO	873	40 nM	Up to 1.3 mM	0.48	2012, [46]
CuO nanoparticles/GCE	1430	5 μM	Up to 6 mM	0.40	2013, [47]
CuO nanosheets/Gold coated glass	520	0.1 μM	Up to 10 mM	0.50	2013, [48]
CuO nanospheres/GCE	405	1 μM	Up to 2.55 mM	0.60	2008, [49]
CuO nanoflowers/GCE	2657	1.71 μM	Up to 5 mM	0.50	2013, [50]
CuO nanourchins/GCE	2682	1.52 μM	Up to 3 mM	0.50	2013, [51]
Sandwich-structured CuO/GCE	5343	1 μM	Up to 3.2 mM	0.60	2013, [52]

GCE: glassy carbon electrode, ITO: Indium tin oxide coated glass, FTO: Fluorine tin oxide coated glass, LOD: Limit of detection.

Table 2
Other metal compound based NEGs and their detection performances. Measurements were performed using amperometric technique.

Electrode matrix	Sensitivity/μA mM^{-1} cm^{-2}	LOD	Linear range	Applied potential/V	Publication year and reference
NiO employed Ni foam	6658	0.46 μM	Up to 5.5 mM	0.55	2013, [55]
NiO microfibers/FTO	1785	33 nM	Up to 0.27 mM	0.50	2011, [56]
Fe_2O_3 nanowire arrays/GCE	728	6 μM	Up to 8 mM	0.52	2011, [58]
CoO nanorods/FTO	572	58 nM	Up to 3.5 mM	0.50	2011, [59]
Co_3O_4 nanoparticles/GCE	521	0.13 nM	Up to 0.8 mM	0.59	2012, [60]
RuOx-Prussian Blue/GCE	6.2	40 μM	Up to 20 mM	1.10	2005, [61]

GCE: glassy carbon electrode, FTO: Fluorine tin oxide coated glass, LOD: Limit of detection.

was found to be limited because of their poisoning sensitivity to chloride.

Noh et al. [62] explored the hierarchical nanostructures present in Cu/Co alloy (molar ratio of 1:1) dendrite based electrodes, which were prepared via electrodeposition on a GCE. The alloys have shown electrocatalytic activity to the oxidation of glucose and also for the reduction of H_2O_2. The authors found that the Co^{2+} ions in the alloy are the main contributors to the oxidation of glucose, with the Cu^{+} ions providing limited assistance in the oxidation. Another alloy based electrode, Ni/Ag, prepared by Miao et al. [63], exhibited an amperometric response to changes in the glucose concentration when the Ni:Ag ratio was 8:2. They also demonstrated that the Ag improves the electrocatalytic performance of the Ni at lower potentials.

Some recent studies investigated the use of electrochemical methods for the fabrication of alloys. A mesoporous Pt/Au alloy film was electrodeposited on an Au coated Si substrate by Li et al. [64] via a square-wave potential program. Through tuning the composition of the Pt and Au species in precursor solutions, Pt/Au alloy films with different compositions were synthesized. Fig. 7. shows the SEM images of the prepared Pt/Au alloy films with different molar ratios, in which the observed mesopore size reaches about 7–8 nm. Among the various Pt:Au ratios, the $Pt_{51}Au_{49}$ alloy film based glucose sensors were most effective, as those were capable of measuring glucose in the concentration range of 6.0 μm to 11 mM with a sensitivity of 352 μA mM^{-1} cm^{-2} and an LOD of 6 μM [64].

More developments of alloy based NEG sensors were brought about through the implementation of various nanostructured composites. Some researchers have investigated the impact that alterations in tunable properties such as surface morphology, pore size, and overall pore microstructure can have on the electrocatalytic properties of alloy nanomaterials. In one such study by Cao et al. [65], it was found that by linking dispersed nanoparticles it is possible to improve the electrochemical activity and durability of Pt-based bimetal nanomaterials. Specifically, they synthesized Pt/Cu nanochains through wet chemical processing and, once chains of a standard stoichiometry were obtained, different atomic ratios of Pt/Cu alloys were yielded through a dealloying process. The prepared, modified $Pt_{75}Cu_{25}$ alloy nanochain-based glucose sensor electrode showed optimized performance as compared to similar alloys, with a sensitivity of 135 μA mM^{-1} cm^{-2} [65].

Shim et al. [66] prepared a nanoporous gold/ruthenium nanocomposite on a GCE substrate and with chitosan (GCE/np Au–Ru/CHIT) as the coating membrane. The np Au–Ru nanocomposites were synthesized by galvanic replacement reaction between Co NPs and an Au precursor, and the resulting Au:Ru weight ratio was 84:16. The GCE/np Au–Ru/CHIT electrode showed a linear amperometric response to glucose in the concentration range of 0–6 mM, with an overall sensitivity of 240 μA mM^{-1} cm^{-2} [66].

By a magnetic-field-assisted (MFA) layer-by-layer (LBL) method, Shao et al. [67] fabricated CoFe layered double hydroxide (CoFe-LDH) nanoplatelets along with manganese porphyrin (Mn-TPPS) on ITO substrates. The schematic strategy of their fabrication is shown on Fig. 8. With the assistance of an external magnetic field, positively charged CoFe LDH, with nanoplatelets as building blocks, were assembled alternately with negatively charged 5,10,15,20-tetrakis(4-sulfonatophenyl) porphinatomanganese(III) (Mn-TPPS) on a pretreated ITO substrate. The resulting $(CoFe\text{-}LDH/Mn\text{-}TPPS)_n$ multilayer ultrathin film (n: the number of bilayers) based glucose sensor showed optimal electrochemical activity when the bilayer number was six and the applied magnetic field was 0.5 T [67].

2.2.2. Metal oxide composite based glucose sensors

In addition to noble metal and alloy based glucose sensors, researchers have investigated various metal oxide composites [13]. These materials have been largely investigated due to the fact that they are inexpensive, can integrate advantages of both metals and metal oxides, and can be fabricated via a variety of methods. Herein, the most recent studies on nano- and micro-structured metal oxide composite-based NEG sensors are discussed, covering the last few years. Namely, the most advanced research on glucose sensors based on 1) metal/metal oxide composites, 2) metal oxide/metal oxide composites, and 3) metal/metal composites. The performances of the NEG sensors in this group are shown in Table 4.

2.2.2.1. Metal/metal oxide composites. In order to combine the high conductivity of metals with the excellent electrocatalytic activity of metal oxides, much of the recent research has focused on metal/metal oxide composites. In the composites, the metals or metal oxides are chosen in such a way that: 1) the substrate material has a high electron transfer rate and is a stable support for the coating material and 2) the loading material enhances the surface area and electrocatalytic activity of the sensor. Zhang et al. [69] proposed an NEG sensor based on a Cu substrate coated with CuO nanowalls. The CuO nanowalls were grown via seed-mediated growth from vertical arrays of CuO nanoplatelets present on the surface of the Cu substrate. These prepared nanocomposites were

Table 3
Alloy or bimetallic composite based NEGs and their detection performances. Measurements were performed using amperometric technique.

Electrode matrix	Sensitivity	LOD	Linear range	Applied potential/V	Publication year and reference
Ag–Ni alloy/GCE	6.48 μA mM^{-1}, 2.88 μA mM^{-1}	0.49 μM	1–9.89 μM, 19.68–106.89 μM	0.45	2013, [63]
Pt–Au alloy/Si substrate	352 μA mM^{-1} cm^{-2}	6.0 μM	6.0 μM–11 mM	0.3	2013, [64]
Cu–Co alloy/	–	0.1 μM	0.5 μM–14 Mm	0.65	2012, [62]
Au–Ru nanocomposite/Chitosan/GCE	240 μA mM^{-1} cm^{-2}	1.7 μM	0–6 mM	−0.1	2011, [66]
CoFe-LDH (layered double hydroxide)/manganese porphyrin (Mn-TPPS)/ITO	66.3 μA mM^{-1} cm^{-2}	0.79 μM	0.1–15 mM	0.6	2011, [67]
Pt–Cu nanochains/GCE	135 μA mM^{-1} cm^{-2}	2.5 μM	0.01–14 mM	−0.01	2013, [65]

GCE: glassy carbon electrode, ITO: Indium tin oxide coated glass, LOD: Limit of detection.

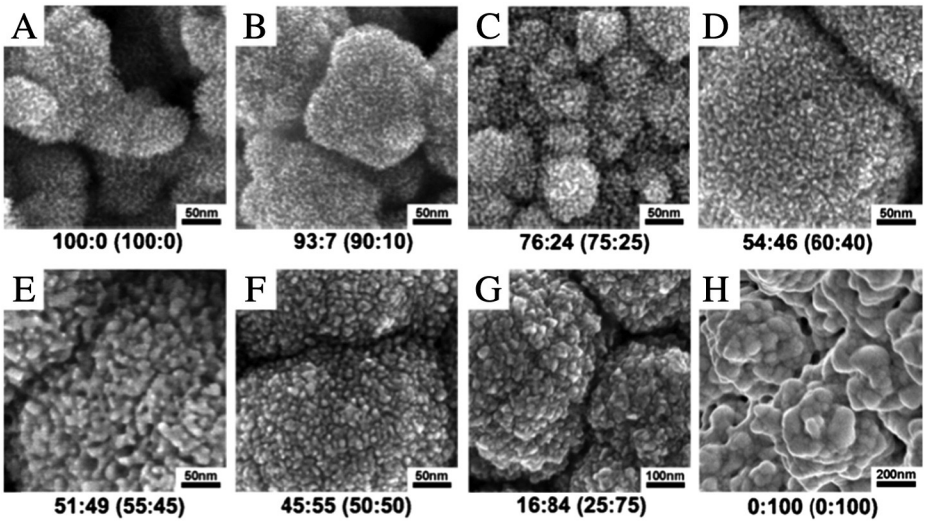

Fig. 7. SEM images of Pt–Au alloy films with different compositional ratios. The product compositions of Pt/Au in the films are noted and the corresponding compositional ratios of the used precursor solutions are also given in parentheses. Reprinted with permission from [64] C. Li, H. Wang and Y. Yamauchi, Chem. Eur. J. **19**, 2242 (2013). © 2013 WILEY-VCH Verlag GmbH & Co. KGaA, Weinheim.

shown to improve electron transfer between the glucose and the CuO nanowalls/Cu modified GCE as proven by electrochemical impedance spectroscopy (EIS) measurements. The amperometric response showed the resulting product had a linear response over the range of 0.05 mM to 10 mM concentrations, with a sensitivity of 5563 μA mM^{-1} in phosphate buffered solution with a pH of 9.2 [69].

Other oxidation states of copper oxide have been studied, specifically Cu_2O/Cu nanocomposites. Wang et al. [70] reported the fabrication of Cu/Cu_2O hollow microspheres (HMs) via in-situ over-reduction under solvothermal conditions. The purpose of these microspheres was to apply a coating on the surface of the GCE and enhance glucose sensing capabilities. They found that the Cu_2O microcubes transform to hollowspheres (Cu_2O HMs) and then to microspheres upon increasing the reaction temperature. However, also upon increasing the reaction temperature, Cu_2O was gradually reduced to Cu. Due to its capacity to increase the reaction area as well as the conductivity, the Cu/Cu_2O HMs modified GCE has proven to have higher catalytic activity than pure Cu_2O microspheres or microcubes with respect to the oxidation of glucose. Also on a Cu substrate, porous NiO nanoplates have been grown by the dehydration of a Cu/$Ni(OH)_2$ precursor. Zhang et al. [71] prepared of an amperometric glucose sensor based on these Cu/NiO nanocomposite modified GCEs which exhibited a sensitivity of 156.4 μA mM^{-1} cm^{-2} and an LOD of 0.5 μM. Fang et al. [72] synthesized composites of Ag_2O nanowalls (Ag_2O NWs), which consisted of packed nanoplates on a Cu substrate. The prepared Cu/Ag_2O NWs/GCE not only exhibited an amperometric response to glucose detection, it also effectively avoided the interferences from fructose, which is the isometric of glucose. Ahmad et al. [73] synthesized CuO nanoparticles and generated a solution consisting of ink mixed with water, ethanol, iso-propanol, and diethylene glycol along with the prepared 20 wt.% CuO NPs. Then, the NEG sensor was fabricated by loading Inkjet-printed copper oxide nanoparticles (CuO NPs) on an Ag surface. The CuO NPs/Ag based sensor produced a sensitivity of 2762.5 μA mM^{-1} cm^{-2} with a linear detection range from 0.05 to 18.45 mM and an LOD of 0.5 μM [73].

Although all of the previously reported metal/metal oxide composites have been based on the same structure, specifically a metal substrate coated by a nano- or micro-structured metal oxide, other systems can also be used where the metal serve as the electrocatalyst coated on the metal oxide substrate. Yu et al. [74] developed novel NEG sensors using a Ni nanoparticle-loaded TiO_2 nanotube array (Ni NPs/TiO_2 NTs). Here the TiO_2 NTs are the substrate, serving as the supporting matrix for the electrocatalytic Ni NP coating. The properties of the TiO_2 NTs, such as large specific surface area, high electron transfer rate, and superior bio-affinity make this arrangement ideal. These

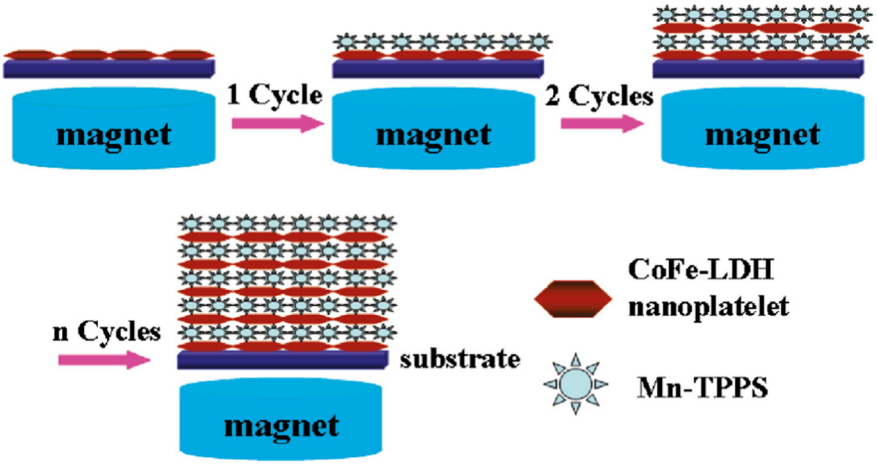

Fig. 8. Schematic representation of the MFA LBL assembly of $(CoFe\text{-}LDH/MnTPPS)_n$ films. Reprinted with permission from [67], M. Shao, X. Xu, J. Han, J. Zhao, W. Shi, X. Kong, M. Wei, D. G. Evans and X. Duan, Langmuir. **27**, 8233 (2011). © 2011, American Chemical Society.

Table 4
Metal oxide composite based NEGs and their detection performances. Measurements were performed using amperometric technique.

Electrode matrix	Sensitivity	LOD	Linear range	Applied potential/V	Publication year and reference
Metal/metal-oxide (M/MO) composites					
Cu–Ag_2O nanowalls/GCE	298.2 μA mM^{-1}	0.01 mM	0.2–3.2 mM	0.4	2009, [72]
Cu–CuO nanowalls/GCE	0.5563 μA mM^{-1}	0.05 μM	0.05 μM–10 μM	0.1	2010, [69]
Cu–Cu_2O hollow microspheres/GCE	33.63 μA mM^{-1}	0.05 μM	0.22–10.89 mM	0.45	2011, [70]
Cu–NiO nanocomposite/GCE	171.8 μA mM^{-1}	0.5 μM	Up to 5 mM	0.4	2011, [71]
CuO nanoparticles/Ag	2762.5 μA mM^{-1} cm^{-2}	0.5 μM	0.05 to 18.45 mM	0.6	2013, [73]
Ni nanoparticles (NPs)/TiO_2 nanotubes (NTs)	700.2 μA mM^{-1} cm^{-2}	2 μM	0.004–4.8 mM	0.6	2012, [74]
Metal oxide/metal oxide (MO/MO) composites					
CuO–TiO_2 nanotube arrays on Ti foil	79.79 μA mM^{-1} cm^{-2}	1 μM	Up to 2 mM	0.5	2011, [77]
NiO–CuO nanowire arrays on Ti substrate	1600 μA mM^{-1} cm^{-2}	0.1 μM	0.1–1200 μM	0.42	2012, [76]
CuO–NiO microfibers	3165.53 μA mM^{-1} cm^{-2}	1 nM	3 μM–0.51 mM	0.5	2011, [75]
CuO and Pt nanostructure/Ta_2O_5 nanoporous honeycomb	160 μA mM^{-1} cm^{-2}	1 μM	Up to 31 mM	0.7	2013, [78]
Metal/metal compound (M/MC) composites					
Co–CoOOH nanosheet on Au plate	967 μA mM^{-1} cm^{-2}	10.9 μM	Up to 0.5 mM	0.5	2012, [79]
Cu–Cu_2S nanocomposite	361.58 μA mM^{-1}	0.1 μM	2 μM–8.1 mM	−0.1	2012, [81]
Cu–CuS nanotubes	3135 μA mM^{-1} cm^{-2}(lower range), 2205 μA mM^{-1} cm^{-2}(higher range)	45 nM	0.2 mM–2.5 mM, 2.5 mM–6 mM	0.45	2013, [80]
Perovskite $LaTiO_3$–$Ag_{0.2}$ (LTA)/GCE	784.14 μA mM^{-1} cm^{-2}	210 nM	2.5 μM–4 mM	0.7	2013, [82]

GCE: glassy carbon electrode, LOD: Limit of detection.

modified NEGs were prepared by the anodic growth of TiO_2 NTs on a Ti foil, followed by annealing to form oxygen vacancies on the surface of the TiO_2 NTs, after which the Ni NPs were deposited via pulse electrodeposition onto the TiO_2 NTs. The formed Ni-NPs/TiO_2 NTs electrode displayed good electrocatalytic performance at an applied potential of 0.6 V with a sensitivity of 700.2 μA mM^{-1} cm^{-2} [74]. The cyclic voltammetric (CV) curve and the glucose sensing mechanism of the prepared electrode are shown in Fig. 9.

2.2.2.2. Metal oxide/metal oxide composite. Based on the drive to produce low-cost electrode materials, an entirely metal oxide system is desirable. Due to their low production costs and ease of fabrication, metal oxides have long been researched. In an effort to expand on synergically catalytic effects of different metal oxides, metal oxide/metal oxide composites have been proposed for NEG sensors. Such publications have focused on designing sensing materials, such as nanowires, nanoarrays, and microfibers, with improved properties [11–13].

The research performed by Cao et al. [75] investigated the use of CuO/doped NiO composite microfibers (CuO/NiO MFs) deposited on a modified FTO substrate. The CuO/NiO MF/FTO exhibited an LOD of 10^{-9} M, with a sensitivity of 3165.53 μA mM^{-1} cm^{-2} [75]. These were fabricated by electrospinning and subsequent calcination, which imparted a tight adhesion between the composite microfibers and the surface of the FTO. After these steps, they introduced more Ni^{3+} in the

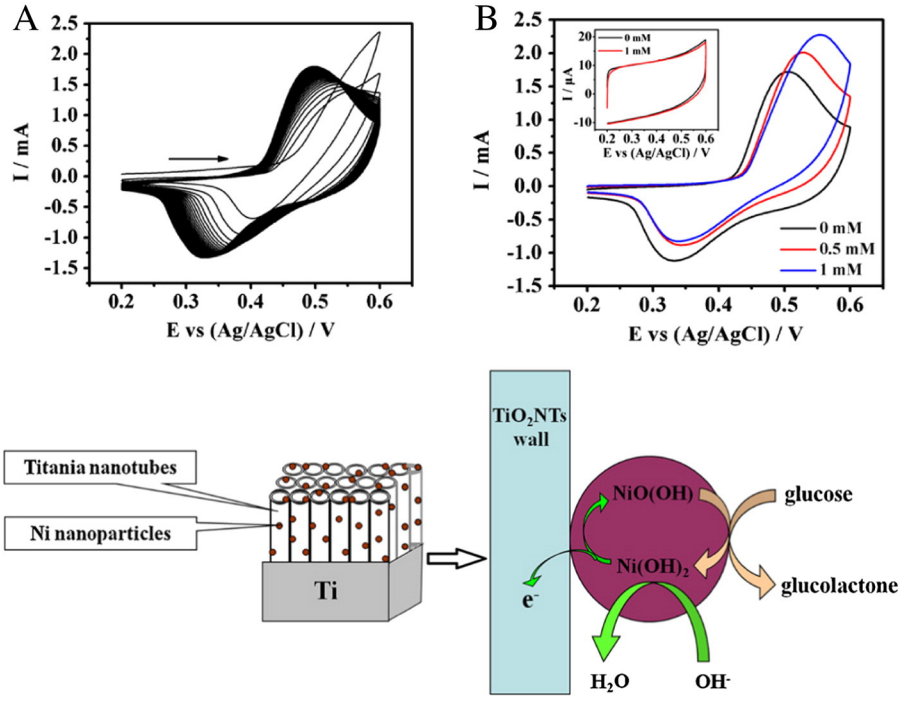

Fig. 9. Top: (A) Cyclic voltammetric (CV) curve of the as-prepared Ni NPs/TiO_2 NTs GCEs in a 0.1 M NaOH solution at the scan rate of 50 mV s^{-1} for 50 cycles. (B) CV curve of the activated Ni NPs/TiO_2 NTs in the presence of 0 mM, 0.5 mM, and 1 mM glucose, respectively (all in 0.1 M NaOH solution). Inset shows the CV curves for the TiO_2 NTs in a 0.1 M NaOH solution, both in the absence and presence of 1 mM glucose, the scan rate for which was 50 mV s^{-1}. Bottom: Schematic representation of the activated Ni NPs/TiO_2 NTs structure as well as a schematic of its glucose sensing mechanism. Reprinted with permission from [74], S. Yu, X. Peng, G. Cao, M. Zhou, L. Qiao, J. Yao, H. He, Electrochimica Acta. **76**, 512 (2012). © 2012, Elsevier.

NiO-MFs which provided additional reaction sites on the electrode by doping the CuO. In a similar system, a NEG sensor based on a mixed metal oxide nanowire array coated on a Ti substrate was proposed by Ding et al. [76]. They produced Ni–Cu oxide nanowire arrays by thermal decomposition of a $\{Ni,Cu\}(OH)_2CO_3$ precursor, and found that each prepared nanowire was a matrix embedded with NiO and CuO grains. The electrode exhibited a high sensitivity of 1600 μA mM^{-1} cm^{-2}, an LOD of 0.1 μM, and a linear amperometric response to glucose concentrations ranging from 0.1 to 1200 μM [76]. Despite these promising results, the use of these materials is limited. Particularly, NiO materials are not biocompatible and may cause lung damage in humans. Thus research has moved to biocompatible metal oxides, where TiO_2 is regarded as the most favorable potential metal oxide electrode material for NEG sensors.

Luo et al. [77] proposed the use of CuO NF/TiO_2 NT arrays as electrodes for glucose sensors, as TiO_2 nanotubes (TiO_2 NTs) possess many advantages, such as large surface area, excellent semiconducting properties, low cost, stability, and have numerous active sites for the growth of CuO nanofibers (CuO NFs). The CuO on the nanotube functioned as an electron transfer mediator in the oxidation of glucose while the TiO_2 substrate provided a high electron transfer rate. At an applied potential of 0.5 V, the CuO NF/TiO_2 NT electrode arrays had a linear range response to concentrations of glucose up to 2 mM with a sensitivity of 79.79 μA mM^{-1} cm^{-2} and an LOD of 1 μM [77]. They also evaluated the selectivity of the prepared electrode to glucose with interferences, and found that the amperometric response of the interfering species is negligible, as shown in Fig. 10.

2.2.2.3. Metal/metal compound composites. Similar to previous sections, metal/metal compound composites have seen a spike in interest over the last several years. A NEG sensor based on a CoOOH nanosheet array deposited on a cobalt substrate has been prepared by Lee et al. [79]. However, the amperometric detection of glucose was only linear for concentrations of glucose in the range of 0 to 0.5 mM [79] and thus further investigation is needed to widen this sensitivity range. In a separate study, CuS nanotubes, which acted as electrocatalysts towards glucose, were synthesized in-situ on a Cu electrode by Qian et al. [80]. The detection signal exhibited an LOD of 45 nM, and was linearly dependent on the glucose concentration, exhibiting two main regions of distinct linear behavior. The lower linear range was for the concentrations between 0.2 mM and 2.5 mM, with a sensitivity of 3135 μA mM^{-1} cm^{-2}. The higher linear range, for concentrations ranging from 2.5 mM to 6 mM, exhibited a sensitivity of 2205 μA mM^{-1} cm^{-2} [80].

Using Cu as the electrode, chalcocite Cu_2S nanoplates were grown on a Cu rod by Zhang et al. [81] via an etching method. The prepared

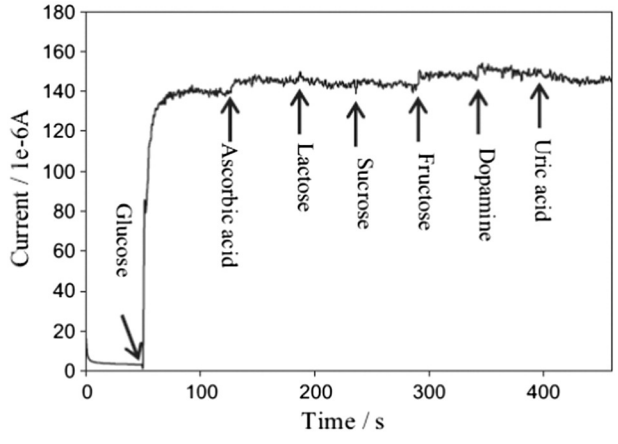

Fig. 10. Amperometric curve of a CuO/TiO_2 electrode with successive addition of 1.0 mM glucose, 0.10 mM ascorbic acid, lactose, sucrose, fructose, dopamine, and uric acid in 0.10 M NaOH solution at 0.50 V. Reprinted with permission from [77], S. Luo, F. Su, C. Liu, J. Li, R. Liu, Y. Xiao, Y. Li, X. Liu and Q. Cai, Talanta. **86**, 157 (2011). © 2011, Elsevier.

Cu/Cu_2S composites exhibited a sensitivity of 361.58 μA mM^{-1}, with an LOD of 0.1 μM. Moving away from more traditional metal oxides, in an investigation into alternative electrode materials, a kind of new inorganic perovskite-type oxide composite was employed by Wang et al. [82]. They fabricated the perovskite $LaTiO_2$–$Ag_{0.2}$ (LTA), together with a modified glassy carbon electrode (LTA-GCE). The perovskite type materials possess many intriguing properties such as ferroelectricity, superconductivity, charge ordering, and high thermopower. Specifically, the perovskite structure can accommodate a number of different metallic ions as well as various anions. Due to this, many perovskite type compounds have been used as sensors and catalyst electrodes in electrochemical fields. In composition of the LTA-GCE, Ag ions act as the oxidizing electrocatalysts, which reacted with glucose to form glucolactone. And the LTA− GCE showed an LOD of 2.1×10^{-7} M and a sensitivity of 784.14 μA mM^{-1} cm^{-2} in the range of 2.5 μM–4 mM [82].

2.2.3. Polymer modified composites

In enzymatic glucose sensors, polymers are used for enzyme immobilization at the electrode surface [83,84]. While in NEG sensors, polymers are mainly used as: a binding mediator between the substrate and the glucose; or as a conductive substrate; or as a modified membrane for enhanced selectivity towards glucose, example of which will be detailed in the following subsections (as shown in Table 5).

Pandya et al. [85] fabricated colorimetric glucose sensors using Au NP complexes, which were functionalized using calix(4)arene boronic acid, (pSC4BA modified Au NPs). These devices were able to selectively detect glucose based on the capacity of the formed molecular receptor to reversibly bind with diol-containing compounds, via boronic acid-diol interactions. The colorimetric response was linearly proportional to the concentration of glucose for concentrations in the range of 5–100 nM with an LOD of 4.3 nM [85]. In this polymer modified composite, the calix(4)arene boronic acid acted as a binder between the glucose and the Ag NPs, and the Ag NPs detected the glucose via a shift in the surface plasmon peak of the UV–vis spectrum.

In using polymers for substrate applications, Çiftçi et al. [86] introduced conductive poly(3-octylthiophene) (POT) as a substrate and immobilized a surface-functionalized-self-assembled monolayer (SAMs) of gold nanoparticles on the surface through hydrophobic forces. The SAMs consisted of 11-mercaptoundecanoicacid (MUA), 4-mercaptophenyl boronic acid (MPB), and 1-decanethiol (DT) on hydrophobic substrates. Since the close-packed SAMs provided effective blocking of the underlying platinum, they proposed that the SAMs (consisting of MPB) could function as a potentiometric glucose detector. The POT/Au/SAM (MPB) based potentiometric NEG sensor, as shown in Fig. 11, behaved linearly in the concentration range of 5–30 mM [86].

Another example of using conducting polymers for substrate applications was introduced by Meng et al. [87]. Specifically, they used a polypyrrole (PPy) nanowire, with an ordered chain structure and a high aspect ratio as the electrode material. They fabricated Cu_xO (CuO and Cu_2O composite) nanoparticle modified PPy nanowires by in-situ electrodeposition and electrochemical oxidation. After the modified nanowires were fabricated, they were electrodeposited on an Au base. The Cu_xO/PPy/Au electrode showed a linear amperometric response towards glucose in concentrations up to 8 mM concentrations, with a sensitivity of 232.22 μA mM^{-1} cm^{-2} and an LOD of 6.2 μM [87].

In the final application of polymeric materials previously mentioned, polymers can be applied as membranes or coating materials in electrochemical biosensors. Some of the more commonly used materials include Nafion, polyurethane, polyethylene glycol (PEG), and hydrogels [28,83]. One such example, an electrode based on the structure of a permselective over-oxidized polypyrrole (OPPy) film, which was electrodeposited on Pd nanoparticles (Pd NPs)/Silicon microchannel plate (Si MCP) array, was recently fabricated by Shi et al. [88]. Due to the formed OPPy film, the electrode surface was effectively resistant to interferences that typically coexist in the presence of glucose. The

Table 5
Polymer modified composite based NEGs and their detection performances. Measurements were performed using amperometric technique.

Electrode matrix	Sensitivity	LOD	Linear range	Applied potential/V	Publication year and reference
calix(4)arene/phenyl boronic acid (CX-PBA) functioned Au nanoparticles (NPs)	–	4.3 nM	5–100 nM	–	2013, [85]
poly(3-octylthiophene) (POT) functioned Au NPs self-assemble monolayer on Pt substrate	–	0.2 mM	5–30 mM	–	2012, [86]
Cu_xO nanoparticles modified polypyrrole(PPy) nanowires on Au substrate	232.22 μA mM^{-1} cm^{-2}	6.2 μM	Up to 8 mM	0.6	2013, [87]
Over-oxidized polypyrrole (OPPy) modified Pd/Silicon microchannel plate (MCP)	0.37 μA mM^{-1} cm^{-2}	2.06 μM	Up to 24 mM	0.08	2011, [88]

LOD: Limit of detection.

vertically aligned MCP was prepared via photo-assisted electrochemical etching, and Pd NPs were fabricated on the MCP via cyclic voltammetry, the resulting structure is shown in Fig. 12. The OPPy modified Pd NPs/Si MCP based NEG sensor performed satisfactorily with an LOD of 2.06 μM, a sensitivity of 0.37 μA mM^{-1} cm^{-2} and the response was linear in the range of 0–24 mM at the applied potential of +0.08 V [88].

Another commonly used polymer is Nafion. It is a perfluorosulfonic acid based polymer that has been widely implemented as a biocompatible coating on electrodes for glucose sensing [89]. Since Nafion has a high cation conductivity and is highly permeable to water, it strongly binds modified materials to electrode substrates [3,90]. The purpose of the Nafion layer is to screen potential interferences from the electrode surface by electrostatic repulsion from the negatively charged sulfonate groups of the Nafion [91,92].

2.3. Carbon micro- or nano-material based glucose sensors

Carbon based substrates have been universally used for the fabrication of electrochemical biosensors due to their large electronic conductivity and the fact that they are generally electrochemically inert [93]. With all of the interest in cutting-edge nanotechnologies, numerous NEG sensors based on carbon nanomaterials have been developed (see Table 6). Thus, various carbon materials such as carbon nanotubes, carbon nanofibers, graphene, doped diamond-like materials, carbon black, and nanodiamonds, have all garnered significant interest [9].

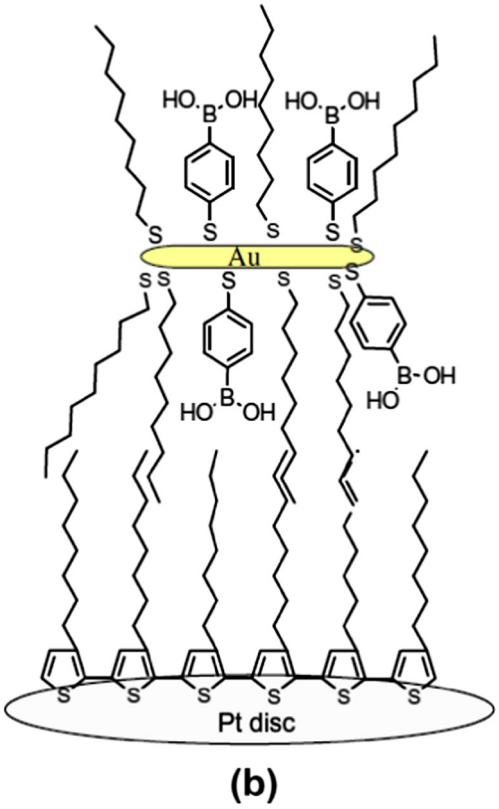

Fig. 11. Schematic illustration of POT-Au-SAM (MUA) structures. Reprinted with permission from [86], H. Çiftçi and U. Tamer, Reactive & Functional Polymers. **72**, 127 (2012). © 2012, Elsevier.

2.3.1. Carbon nanotube

Carbon nanotubes (CNTs) have a high surface area, good mechanical properties, and excellent electrical and thermal conductivities [9,93]. For these reasons, CNTs have drawn a lot of attention in recent years, and many researchers have begun to apply CNTs in various electrical biosensors. The improved performance is attributed to their one-dimensional hollow tubular nano-chemistry, which is responsible for the efficient capture and promotion of electrons transferred from the analyte to the electrode surface [93]. Most of the CNT based NEG sensors are functionalized through combination with metal or metal oxide nanostructured materials. Tremendous research has been conducted on the different deposition methods to possibly connect CNTs to the electrode materials [9,94].

The research of Dung et al. [95] demonstrated that CuO/SWCNT (Single-walled CNTs) composites formed by a co-arcdischarge method have high potential for glucose detection, even better than that of pure CuO or SWCNT sensors. The CuO/SWCNT electrode showed a good linear response to glucose detection in the concentration range from 0.05 to 1800 mM, with a relatively high sensitivity of 1610 μA cm^{-2} mM^{-1} [95]. The synergetic effect of the composite was attributed to the high conductivity network of the highly porous nanowires. Similarly, a multi-walled carbon nanotube (MWCNT) array coated with CuO nanoparticles was fabricated by Jiang et al. [96]. They prepared the MWCNTs on a thin Ta foil and then coated the nanotubes with CuO by sputtering deposition using a copper target under the flow of Ar and O_2. The as-prepared electrode exhibited a sensitivity of 2596 μA mM^{-1} cm^{-2} to glucose at an applied potential of +0.40 V [96].

Yang et al. [97] used CuO nanoleaves (CuO NLs) to decorate MWCNTs in order to produce a novel electrode to facilitate glucose oxidation. Sodium dodecyl sulfate (SDS) was used as a template to deposit CuO on MWCNTs. After dispersion of the CuO NLs in the SDS solution, the MWCNTs were adsorbed using the SDS, which extracted Cu^{2+} from solution. The Cu^{2+} was attached to the outward flanges of the SDS by a static interaction with the dodecyl sulfonic group, thereby forming the desired product. According to the SEM characterization, the MWCNTs were described as “branches” or “nerves” connecting to CuO NLs. Other than CuO, additional metal oxides have also been coated on the carbon nanotubes by electrodeposition and used as NEG sensors. For example, Chen et al. [98] fabricated MnO_2/MWNTs nanocomposites for which the CV behavior of the modified electrode is shown in Fig. 13.

Some researchers also incorporated alloys or bimetallic particles on CNTs for making NEG sensors. Xiao et al. [99] reported the use of bimetallic PtM (M = Ru, Pd, and Au) nanoparticles on carbon nanotubes, deposited by an ultrasonic electrodeposition method. Another study was performed by Liu et al. [100], who studied the deposition of gold and copper alloys on the defect sites of CNTs by a spontaneous reduction among $AuCl^{4-}$, Cu^{2+}, and oxygen-containing functional groups. The capacity of these nanostructures to detect glucose was demonstrated, as these devices had a linear range response to glucose concentrations of 0.08–9.26 mM with an LOD of 4 μM and the sensitivity of 22 μA mM^{-1} [100].

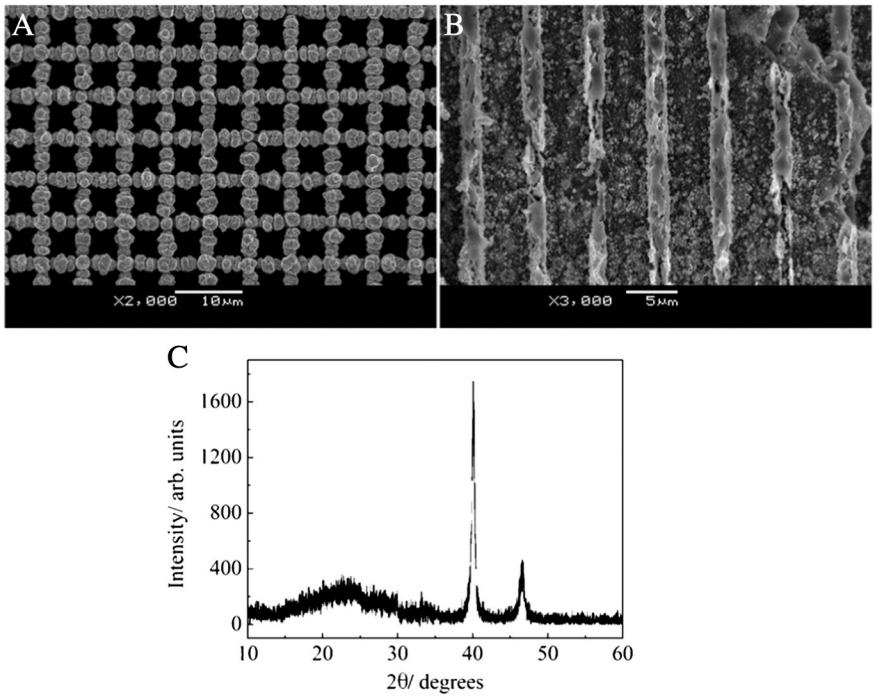

Fig. 12. SEM image of an OPPy modified Pd/Si MCP electrode: (a) top view, (b) cross section, and (c) X-ray diffraction pattern of the OPPy modified Pd/Si MCP electrode. Reprinted with permission from [88], J. Shi, P. Ci, F. Wang, H. Peng, P. Yang, L. Wang, S. Ge, Q. Wang and P. K. Chu, Biosensors and Bioelectronics. **26**, 2576 (2011). © 2011, Elsevier.

Table 6
Carbon micro- or nano-material based NEG sensors and their detection performances. Measurements were performed using amperometric technique.

Electrode matrix	Sensitivity	LOD	Linear range	Applied potential/V	Publication year and reference
Carbon nanotubes (CNTs)					
CuO/SWCNTs/ITO	1610 μA mM^{-1} cm^{-2}	50 nM	0.05–1800 μM	0.45	2013, [95]
CuO nanoparticles/CNTs on Ta foil	2596 μA mM^{-1} cm^{-2}	0.2 μM	Up to 1.2 mM	0.40	2010, [96]
CuO nanoleaves–MWCNTs/	664.3 μA mM^{-1} cm^{-2}	5.7 μM	Up to 0.9 mM	0.35	2012, [97]
Au Cu alloy nanoparticles/CNTs on graphite substrate	22 μA mM^{-1}	4 μM	0.08–9.26 mM	0.34	2010, [98]
MnO_2/MWCNTs on Ta substrate	33.19 μA mM^{-1}	–	Up to 28 mM	0.30	2008, [98]
Cu nanoparticles/MWCNTs	922 μA mM^{-1} cm^{-2}	2 μM	0.5–7.5 mM	0.63	2013, [99]
$Ni(OH)_2$ nanospheres/polyimide/CNT	2071.5 μA mM^{-1} cm^{-2}	0.36 μM	1.0 μM to 0.8 mM	0.60	2013, [102]
Pt nanoparticles/CNTs/GCE	–	28.0 μM	28.0 μM–46.6 mM	−0.40	2011, [103]
Pyrene-1-boronic acid functioned CNTs	–	300 nM	1 μM–100 mM	–	2013, [104]
Pt Ir nanoparticles/MWCNT	206 μA mM^{-1} cm^{-2}	0.5 μM	1–1000 μM	0.1	2013, [105]
Graphene					
Cu_2O nanocubes/graphene sheets/GCE	–	3.3 μM	0.3–3.3 mM	0.60	2013, [107]
NiO/DNA-dispersed graphene hybrid/GCE	9 μA mM^{-1} cm^{-1}	2.5 μM	Up to 8 mM	0.60	2012, [108]
Pt nanoflowers/graphene oxide/GCE	1.26 μA mM^{-1} cm^{-2}(lower range), 0.64 μA mM^{-1} cm^{-2}(higher range)	2 μM	2 μM–10.3 mM, 10.3 mM–20.3 mM	0.47	2013, [109]
PtAu–MnO_2 binary nanocomposites/graphene paper/	58.54 μA mM^{-1} cm^{-2}	0.02 mM	0.1 mM–30.0 mM	0	2013, [112]
Co_3O_4-graphene needle electrode	–	10 μM	50 ~ 300 μM	0.60	2012, [111]
PtNi nanoparticles/Graphene	20.42 μA mM^{-1} cm^{-2}	0.01 mM	Up to 35 mM	−0.35	2011, [110]
Au/thionine/Graphene oxide/GCE	–	0.05 μM	0.2 μM–22 μM–13.5 mM	–	2012, [113]
Other carbon materials					
NiO nanoparticles/orderd mesoporous carbon/GCE	834.8 μA mM^{-1} cm^{-2}	0.65 μM	2–1000 μM	0.55	2013, [115]
Pt–Pd nanoparticles/onion-like mesoporous carbon/Nafion/GCE	0.11 μA mM^{-1} cm^{-2}	0.12 mM	1.5–12 mM	−0.02	2011, [117]
Cu_2O/Carbon Vulcan XC-72/Nafion on graphite substrate	629 μA mM^{-1} cm^{-2}	2.4 μM	Up to 6 mM	0.75	2011, [118]
Ni nanoparticles/Carbon Vulcan XC-72/Nafion on carbon rod	1349.7 μA mM^{-1} cm^{-2}	0.232 μM	–	0.75	2013, [119]
Au nanoflowers/phosphorus doped diamond-like carbon film on Si substrate	20 μA mM^{-1} cm^{-2}	150 μM	0.3–30 mM	<0.1	2012, [120]
$Cu(OH)_2$ nanoflower electrode/boron-doped nanocrystalline diamond layer on Cu substrate	2159.2 μA mM^{-1} cm^{-1}	9 μM	Up to 6 mM	0.50	2012, [122]
$Ni(OH)_2$ modified nitrogen-incorporated nanodiamonds on Si substrate	3.20 mA mM^{-1} cm^{-2} (higher range) 1.41 mA mM^{-1} cm^{-2}(lower range)	1.2 μM	0.02–1 mM, 1–9 mM	0.48	2013, [123]
Cu core/carbon shell (Cu/C) coaxial nanowire/Nafion/GCE	437.8 μA mM^{-1} cm^{-2}	50 nM	Up to 3 mM	0.65	2013, [124]
CuO nanoneedle/graphene/carbon nanofiber/GCE	912.7 μA mM^{-1} cm^{-2}	0.1 μM	1–5.3 mM	0.60	2013, [125]

CNTs: carbon nanotubes, SWCNTs: single-walled carbon nanotubes, MWCNTs: multi-walled carbon nanotubes, ITO: Indium tin oxide coated glass, GCE: glassy carbon electrode, LOD: Limit of detection.

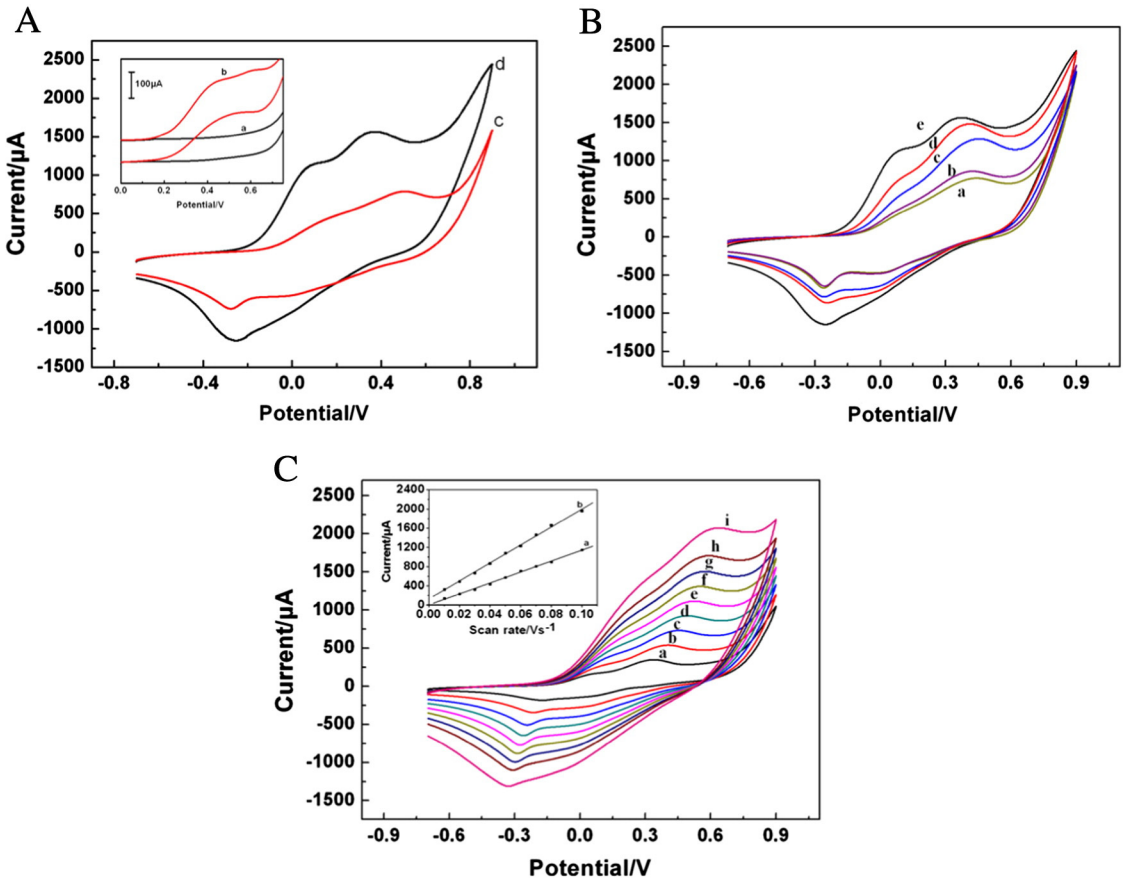

Fig. 13. CV curves of (A) MWNTs (a and b) and MnO_2/MWNTs electrodes (c and d) in the absence (a and c) and presence (b and d) of 10 mM glucose in 0.10 M NaOH solution. Scan rate: 50 mV s^{-1}; (B) MnO_2/MWNTs electrode in 0.10 M NaOH solution containing 2.0, 4.0, 6.0, 8.0, and 10.0 mM glucose (a–e) at 50 mV s^{-1}; (C) A MnO_2/MWNTs electrode at different scan rates (10–100 mV/s) in 0.10 M NaOH solution. Inset is the plot of two oxidative peaks current with different scan rate (10–100 mV/s). Reprinted with permission from [98], J. Chen, W. D. Zhang, J.S. Ye, Electrochemistry Communications. **10**, 1268 (2008). © 2008, Elsevier.

Although electrodeposition methods are very common for fabricating these devices, it has been illustrated by Zhao et al. [101] that similar nanocomposites may be produced using alternative means. Zhao et al. synthesized cubic Cu nanoparticles in conjunction with arc-synthesized multi-walled carbon nanotubes (MWCNTs). They used substrate-enhanced electroless deposition (SEED) and arc-synthesized cylindrical deposition to fabricate an electrode layer that contained an abundance of MWCNTs in order to effectively replace the common GCEs. The schematic of the process and the preparation system are shown in Fig. 14. The SEED technique has the advantage of being capable of continuously synthesizing films by arc-discharge in air at large scales. This prepared sensor exhibited a high sensitivity of 922 μA mM^{-1} cm^{-2} and low detection limit of 20 μM [101]. A glucose sensor-based on the combination of $Ni(OH)_2$ nanospheres and a polyimide/carbon nanotube (PI/CNT) membrane was fabricated by Jiang [102]. The PI/CNT membrane was used to enhance the conductivity and mechanical properties as compared to both ITO and GCE. The $Ni(OH)_2$ was electrodeposited on the PI/CNT membrane at −1.20 V for 5 min [102], and, upon testing, the PI/CNT/$Ni(OH)_2$ films exhibited anodic current enhancement at 0.57 V. This research also shed light on the proposed growth mechanism of nanostructured $Ni(OH)_2$ for hierarchical morphologies in the electroreduction precipitation process, which is shown in Fig. 15.

CNT based nanohybrids have also been achieved through the mediation of protein molecules. A CNT/Pt NP/GCE electrode was prepared by Wei et al. [103]. They investigated the interaction between the CNTs and biomolecules by introducing a protein in the synthesis of the CNT-PtNPs to act as a bio-functional link, a representation of which is shown in Fig. 16. Firstly, Wei et al. prepared the super-water soluble CNT-hemoglobin (HGB) nanofibers by phase-transferring Z-glycine N-succinimidyl ester (Z-Gly-OSu) modified CNTs from toluene to an HGB aqueous solution. Then, the CNT-PtNP nanohybrids were obtained by chemically reducing the $PtCl^{-}_{62}$ ions, which were electrostatically adsorbed onto the CNT-HGB nanofibers in $NaBH_4$ solution. It was demonstrated that the density of the Pt NPs and the water-solubility of CNTs can be manipulated by altering the protein concentration. The CNT/Pt NP modified GCE exhibited a linear response for glucose concentrations of 28.0 μM–46.6 mM [103].

Another promising approach for direct biological detection is the use of carbon nanotube field-effect-transistors (CNT FETs). The combination of FET and CNTs is advantageous for many reasons, such as being able to form a semi-conducting channel using CNTs; enhancing absorption of molecules on the FET surface and allowing manipulation at the molecular level with cells [9]. Lerner et al. [104] developed a CNT based FET functionalized with pyrene-1-boronic acid, and then applied this system for glucose detection. The sensitivity of this CNT FET to the local charge environment facilitated a minimum detection limit of 300 μM [104].

2.3.2. Graphene and graphene oxide

Graphene and its derivatives have attracted significant attention, since first being discovered in 2004, for their potential application as electrochemical biosensors, particularly due to their electrical advantages [9,94,106]. There are three main electrical characteristics driving its use. First, graphene can be referred to as semimetal with a zero-band gap. Secondly, the type of charge carriers in the graphene can be turned by adjusting the gate voltage. And third, the charge carriers are identified as massless Dirac fermions and can move in range of micrometers without scattering at room temperature [94,106]. Graphene

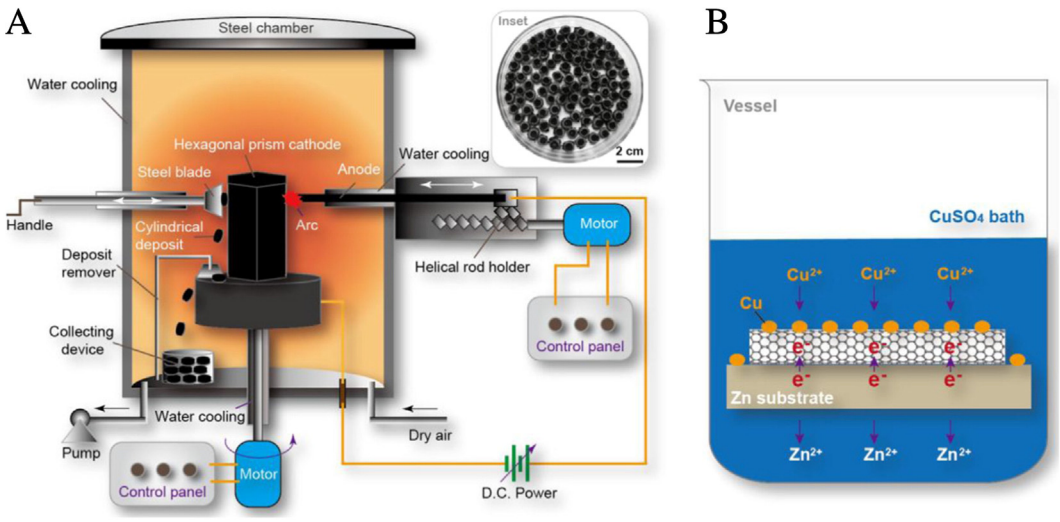

Fig. 14. (A) Schematic of the arc discharge apparatus for continuously prepared cylindrical deposits. The inset shows some cylindrical deposit products. (B) Schematic of Cu nanoparticle deposition on CNTs via the SEED process. Reprinted with permission from [99], J. Zhao, L. Wei, C. Peng, Y. Su, Z. Yang, L. Zhang, H. Wei and Y. Zhang, Biosensors and Bioelectronics. 47, 86 (2013). © 2013, Elsevier.

possesses highly desirable properties, such as its large surface area, low charge-transfer resistance, and fast electron transfer rate. These properties are mainly attributed to the delocalized π bonds above and below the basal plane, as the delocalized electrons create high electrical conductivities and mobilities for graphene within the plane. In addition, the morphology of graphene is quite similar to that of CNTs, as it can be described as an unzipped CNT. Therefore, like in the case of CNTs, it is anticipated that functionalized graphene will show remarkable capacities in glucose detection as it can also be used in conjunction metal nanoparticles or even doped with atomic species [9,106].

In novel studies on the application of graphene in glucose sensors, Liu et al. [107] studied Cu_2O nanocubes, wrapped with graphene nanosheets, as (Cu_2O/GNSs) based NEG sensors. With the Cu_2O/GNs modified electrode, the linear response of amperometric sensing test reached a detection limit of 3.3 μM in a concentration range of 0.3 to 3.3 mM [107]. They found that the graphene served as an additional surfactant during the synthesis of the nanocomposite, thereby reducing the size of the Cu_2O nanocubes and preventing particle aggregation of the Cu_2O, both of which enhanced the electrochemical stability.

The hybrids generated using graphene in conjunction with metal NPs are commonly limited in their capacity to disperse in aqueous solution and this disadvantage has blocked their application in many fields. Therefore, studies have been conducted focusing on uniform dispersion of graphene for NEG sensor applications. The research done by Lv et al. [108] showed that high concentration graphene nanosheet (GNS) suspensions can be obtained via the hybridization of GNSs with ss-DNA (single-strand DNA). They proved that uniform layers of active GNS/NiO can be deposited on GCEs by employing ss-DNA, which enhances the electron transferring in the electrocatalytic reaction process. These GNS/NiO/DNA hybrids demonstrated good glucose detection potential.

Graphene oxide (GO) is also a promising material for the immobilization of a wide range of substances that have the oxygen functional group such as hydroxyl, carboxyl, and epoxy groups on their basal planes and/or on edges [106,109]. For this reason, the hybridization of GO with other nanomaterials has been exploited in NEG sensors due to its improved electrochemical properties. Wu et al. [109] developed a GCE modified with platinum nanoflowers (Pt NFs), and supported on GO for glucose sensing. The modified electrode performed with an LOD of 2 μM, a linear current response to the concentration of glucose ranging from 2 μM to 30 mM, and with two different response regions, one from 2 μM to 10.3 mM with a sensitivity of 1.26 μA mM^{-1} cm^{-2}, and the second from 10.3 mM to 20.3 mM with a sensitivity of 0.64 μA mM^{-1} cm^{-2} [109]. They proved that the synergistic effect of Pt NFs and GO are caused by the edge plane-like defective sites on GO and that these structures show improved electrocatalytic activity towards the detection of glucose.

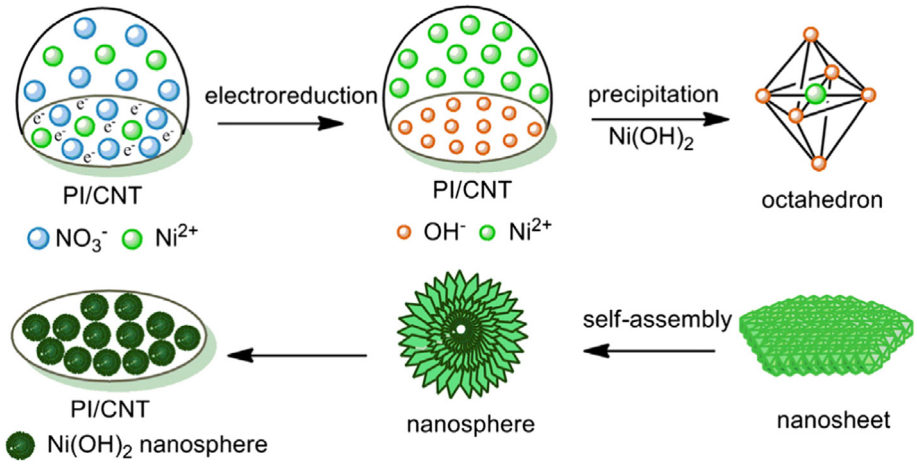

Fig. 15. Proposed growth mechanism for the nanostructures of $Ni(OH)_2$. Reprinted with permission from [102], Y. Jiang, S. Yu, J. Li, L. Jia and C. Wang, CA R B O N. **63**, 367 (2013). © 2013, Elsevier.

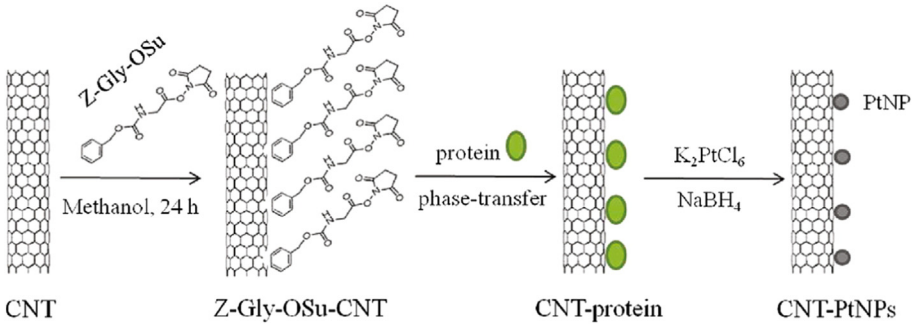

Fig. 16. Model presentation of the protein-directed synthesis of CNT-PtNP nanohybrids. Reprinted with permission from [103], G. Wei, F. Xu, Z. Li and K. D. Jandt, J. Phys. Chem. **115**, 11453 (2011). © 2011, American Chemical Society.

The attachment of metal NPs on graphene substrates can also be prepared by the chemical reduction of GO. Gao et al. [110] reported a one-step ultrasonication-assisted electrochemical synthesis of PtNi nanoparticle-graphene nanocomposites and their application in NEG sensors. They electrodeposited a coating of evenly dispersed PtNi NPs and electrochemically reduced GO (ERGO) simultaneously at a negative potential. In Fig. 17, the SEM images are shown, which revealed the morphologies of the NPs deposited both on the surface of the GO and the SWCNTs, respectively. They demonstrated an enhanced dispersion of NPs on surface of the graphene as compared to the SWCNTs which occurred as a result to the homogeneous spatial distribution of the electrical field along the planar structure of graphene. Gao et al. also confirmed the selectivity, resistance to poisoning, sensitivity, and stability of the prepared PtNi/ERGO modified electrode.

Wang et al. [111] reported the fabrication of a NEG sensor based on a graphene/cobalt oxide hybrid needle-like electrode, constructed on a micropipette tip. The needle electrode was prepared by transferring a chemical vapor deposited graphene strip onto a glass micropipette tip. Co_3O_4 nanoflowers were coated on the graphene needle electrode by electrodeposition, followed by thermal annealing. The unique needle tip sensor enabled detection of glucose in a micro-droplet, with an LOD below 10 μM [111].

A new approach to the co-growth of metals and metal oxides on freestanding carbon substrates was introduced by Xiao et al. [112]. Specifically, they reported a glucose sensor based on the growth of a binary nanocomposite PtAu alloy and MnO_2 on free-standing graphene paper (GP). The GP was formed from graphene nanosheets via mold casting, which allows for control of the thickness and the size of the GP. The fabricated nanocomposites, coral-like PtAu-MnO_2, were grown on the GP through a one-step, template-free electrodeposition, which gave rise to a larger active surface area and more active sites for electrochemical reaction. The characterization images and schematic representation of the electrochemical set up system are shown in Fig. 18.

2.3.3. Other carbon based glucose sensors

Other novel carbon materials can also be decorated with catalytic NPs to enhance electrocatalytic activity, increase the surface area, and improve the rate of mass transport. For example, ordered mesoporous carbon (OMC) possesses a uniform and tailored pore structure with tunable pore diameters in mesopore range, a high specific pore volume, and is chemically inert [114]. Luo et al. [115] constructed an OMC modified GCE (NiO/OMC/GCE), which confirmed that OMC is a suitable matrix to be loaded by nanoparticles. They manipulated the particle size of the NiO NPs, and the NiO NPs nucleated at electroactive sites of OMC during the electrodeposition process. While applying in glucose detection, the resulting sensor determined the level of glucose linearly in 2–1000 μM with an LOD of 0.65 μM, and sensitivity of 834.8 μA mM^{-1} cm^{-2} [115].

Another unique carbon structure, onion-like mesoporous carbon vesicles (MCV) having a uniform distribution of pore size, a high specific surface area, an onion-like lamellar structure, and a large pore volume, was reported by Gu et al. [116]. The MCVs have the potential to be useful as templates for metal nanoparticle coatings. Bo et al. [117] studied the incorporation of PtPd nanoparticles on an MCV. The resulting NEG

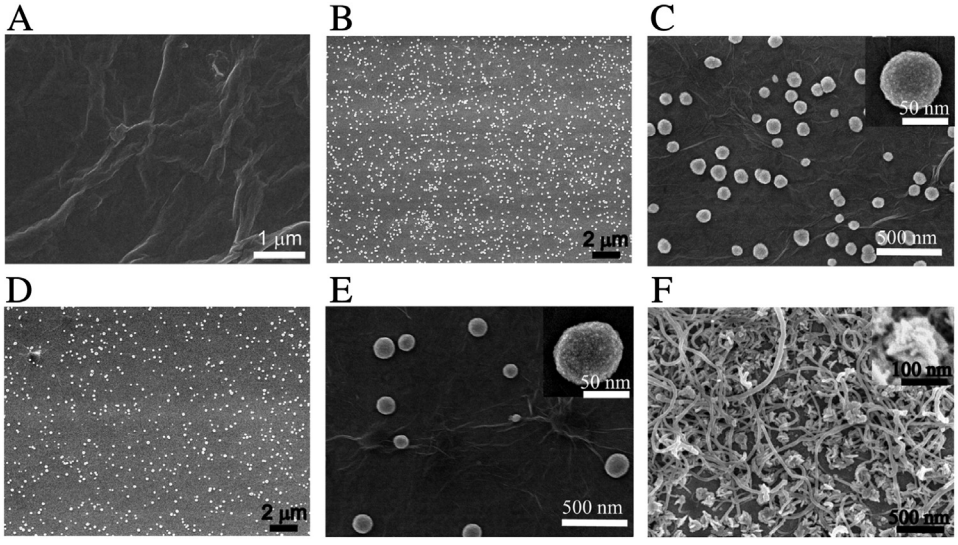

Fig. 17. (A) SEM images of as-synthesized GO films; (B) SEM image of PtNi-ERGO nanocomposites, (D) PtNi-CRGO nanocomposites and (F) PtNi-SWNT nanocomposites. (C, E) Magnified SEM images of B and D, respectively. Reprinted with permission from [110], H. Gao, F. Xiao, C. B. Ching and H. Duan, ACS Appl. Mater. Interfaces. **3**, 3049 (2011). © 2011, American Chemical Society.

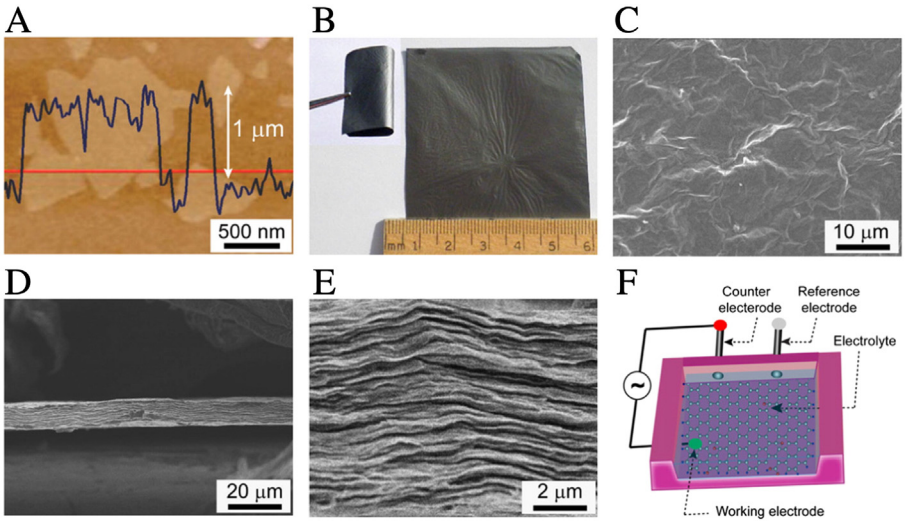

Fig. 18. (A) AFM micrograph of graphene nanosheets, (B) photographs of the same nanosheets, (C) SEM micrographs of top view, (D), (E), and (F) SEM micrograph cross-sectional views of GP. (G) Schematic representation of the assembled electrochemical setup with the location of three electrode system; the working electrode is a contacted GP. Reprinted with permission from [112], F. Xiao, Y. Li, H. Gao, S. Ge and H. Duan, Biosensors and Bioelectronics. **41**, 417 (2013). © 2013, Elsevier.

sensor displayed a rapid current response, which was linear in the range of 1.5 to 12 mM, and produced steady-state signals in 3 s [117].

Carbon black (e.g. Vulcan XC-72), which has the advantages of low cost and high availability, has been used in field of electrochemistry for years. Khatiba et al. [118] developed a NEG sensor based on a Cu_2O/carbon black (Vulcan XC-72) electrode. The coating of Cu_2O NPs was deposited on the surface of carbon black by the impregnation method using $NaBH_4$ as the reducing agent. It was found that different molar quantities of $NaBH_4$ directly affect the morphology of the Cu_2O/carbon black (Vulcan XC-72) composites. In 2013, Hameed [119] constructed nickel nanoparticles (Ni NPs) on Vulcan XC-72 by chemical deposition, with the assistance of microwave irradiation. He found the mode and time of microwave irradiation affected the morphology of the Ni/C powder. Used as glucose sensor, the Ni/C sample showed a linear detection range up to 2.7 mM, an LOD of 0.232 μM, and a sensitivity of 1349.7 μA mM^{-1} cm^{-2} [119].

Other carbon substrates with reproducible surface structure and that are suitable for chemical modification were also studied as electrode materials for glucose detection. Among these, Liu et al. [120] synthesized 3D-flower like phosphorus doped diamond-like carbon (DLC:P) thin films, and then the films were coated by Au nanoparticles via electrochemical deposition to form NEG sensor electrode. Morphology of the nanostructured Au was controlled by altering the electrodeposition potential. Of all the morphologies generated, the nanoflower structured Au obtained at −0.1 V exhibited the highest electrocatalytic activity for glucose electro-oxidation [120].

Boron-doped diamond (BDD) electrodes for electrochemical applications have been the focus of many studies because of their wide potential range, low background current, and mechanical durability [121, 123]. Sim et al. [122] developed an NEG sensor using boron-doped nanocrystalline diamond (BDND) together with a Cu nanoflower electrode of the form $Cu(OH)_2$. Their synthesis strategy was an electrostatic self-assembly seeding method with nanodiamond particles used in conjunction with a hot filament chemical vapor deposition. The BDND/$Cu(OH)_2$/Cu electrode exhibited a linear response for glucose concentrations of 0–6 mM, an LOD of 9 μm and the sensitivity of 2.1592 mA mM^{-1} cm^{-1}[122]. A second classification of nanodiamonds, nitrogen-incorporated nanodiamonds (NND), have likewise garnered recent interests. The experiments conducted by Ko et al. [123] indicated that the as patterned NND film could be coated with nanoscale $Ni(OH)_2$ using electron-beam evaporation to form NND/$Ni(OH)_2$, after which the composites were subsequently deposited on Si substrates. The optimized NND/$Ni(OH)_2$/Si electrode they prepared exhibited enhanced electrocatalytic ability and long-term stability with respect to other glucose sensors.

Zhao et al. [124] produced a one-dimensional copper core/carbon shell (Cu/C) coaxial nanowire as a NEG sensor. The Cu nanowires (Cu NWs) were coated with an amorphous carbon shell through a continuous flow wet-chemistry approach, which is based on catching Cu^{2+} from electroplating wastewater via a hydrothermal carbonization process. Zhao et al. studied different hybrid carbon nanostructure modified GCEs, Cu/C amorphous NWs, Cu/C graphite NWs, and Cu/C amorphous nanoparticles (NPs) modified with MWCNTs. The prepared one-dimensional copper/carbon (Cu/C) core-shell coaxial NWs demonstrated a sensitivity of 437.8 μA mM^{-1} cm^{-2} towards glucose at 0.65 V, with an LOD of 50 nM [124]. It was confirmed that the geometric factors had a high impact on the performance of the electrode, and that the electrocatalytic behavior was enhanced by well-spaced adsorption sites and increasing surface area of the modified electrode.

3. Conclusion

In this review, we have shown that the behavior of most nonenzymatic glucose sensors is a direct function of the electrode material on which the glucose is oxidized. Recent efforts have been focused on exploiting different materials and fabrication processes for these electrodes. In early research studies, metals such as Pt, Au, Ni, Cu, and Ag and compounds such as nickel oxides, iron oxides, cobalt oxides, silver oxides, and ruthenium oxides were used. More recently, the combination of various metals and/or metal compounds, such as alloys and metal/metal oxide composites have been explored for their synergistic effects and excellent electrocatalytic activities. Also, polymer modified composites have been used as electrodes because of their high selectivity and bicompability. In the recent boom of nanotechnology research, unique nanostructures and techniques have been used to bring innovative developments to current glucose sensors. Nanostructured metals or metal oxides offer larger surface area for the oxidation of glucose. The use carbon nanotubes and graphene has also drawn a lot of attention, as the high conductivity of these materials increases the electron transfer rate and therefore improves their sensitivity. Most research with respect to nanotechnology has been focused on the fabrication and integration of nanomaterials to improve the performance of electrochemical NEG sensors.

However, there are still a lot of challenges ahead with respect to utilization in the human body, before the commercialization of these techniques is possible. Most glucose sensors based on novel materials

have been limited due to their poor biocompatibility, high cost, and very time-intensive preparation processes. Thus, there still exists the challenge of exploiting materials with high selectivity, low detection limit, a wide detection range, and fast response time, all while attempting to make these sensors ready for continuous glucose measurement. In the future, research will continue to work towards detecting infinitesimally small concentrations of glucose via different bodily fluids and in forming sensors that are capable of being incorporated in to portable, subcutaneous, and miniaturized implantable devices. Durable and implantable glucose biosensors, in addition to supplying information rapidly and accurately, are envisioned to be used for continuous glucose level monitoring. In an interest to move beyond current electrochemical and optical techniques, spintronic detection techniques have been proposed. Spintronics is a new branch of electronics that have been shown to be more efficient, faster, and consume less electricity than traditional devices. These disciplines can offer another potential approach to fabricate biosensors with enhanced properties. All these requirements urge the continuous exploration to revolutionize the glucose biosensor industry through perfection of NEG sensors.

Acknowledgments

Infrastructural research support from the University of Utah's NSF MRSEC (Award # 1121252) is thankfully acknowledged.

References

[1] G. Danaei, M.M. Finucane, Y. Lu, G.M. Singh, M.J. Cowan, C.J. Paciorek, et al., National, regional, and global trends in fasting plasma glucose and diabetes prevalence since 1980: systematic analysis of health examination surveys and epidemiological studies with 370 country-years and 2.7 million participants, Lancet 378 (9785) (2011) 31.
[2] Global status report on noncommunicable diseases 2010, World Health Organization, Geneva, 2011.
[3] S.P. Nichols, A. Koh, W.L. Storm, J.H. Shin, M.H. Schoenfisch, Chem. Rev. 113 (2013) 2528.
[4] Diabetes Chronic Complications, in: Kenneth M. Shaw, Michael H. Cummings (Eds.), John Wiley & Sons, 2005.
[5] Diabetes Atlas, third edition International Diabetes Federation, 2006.
[6] A. Chen, S. Chatterjee, Chem. Soc. Rev. 42 (2013) 5425.
[7] D.K. Bishop, J.T. La Belle, S.R. Vossler, D.R. Patel, C.B. Cook, J. Diabetes Sci. Technol. 4 (2010) 2.
[8] M. Righettoni, A. Tricoli, Sotiris E. Pratsinis, Anal. Chem. 82 (2010) 3581.
[9] Z. Zhu, L.G. Gancedo, A.J. Flewitt, H. Xie, F. Moussy, W.I. Milne, Sensors 12 (2012) 5996.
[10] K.E. Toghill, R.G. Compton, Int. J. Electrochem. Sci. 5 (2010) 1246.
[11] J. Wang, J. Pharm. Biomed. Anal. 19 (1999) 47.
[12] S. Park, H. Boo, T.D. Chung, Anal. Chim. Acta. 556 (2006) 46.
[13] M.M. Rahman, A.J.S. Ahammad, J.H. Jin, S.J. Ahn, J.J. Lee, Sensors 10 (2010) 4855.
[14] P. Si, Y. Huang, T. Wang, J. Ma, RSC Adv. 3 (2013) 3487.
[15] D. Pletcher, J. Appl. Electrochem. 14 (1984) 403.
[16] L.D. Burke, Electrochim. Acta 39 (1994) 1841.
[17] S. Ernst, J. Heitbaum, C.H. Hamann, J. Electroanal. Chem. Interfacial Electrochem. 100 (1979) 173.
[18] E. Skou, Electrochim. Acta 22 (1977) 313.
[19] Y. Sun, H. Buck, T.E. Mallouk, Anal. Chem. 73 (2001) 1599.
[20] S. Balat, T.D. Chung, H.C. Kim, Anal. Chem. 75 (2003) 3046.
[21] J. Yuan, K. Wang, X. Xia, Adv. Funct. Mater. 5 (2005) 15.
[22] Y.Y. Song, D. Zhang, W. Gao, X.H. Xia, Chem. Eur. J. 11 (2005) 2177.
[23] C.H. Chou, J.C. Chen, C.C. Tai, W. Sun, J.M. Zen, Electroanalysis 7 (2008) 771.
[24] B. Gollas, J.M. Elliott, P.N. Bartlett, Electrochim. Acta 45 (2000) 3711.
[25] A.J. Bard, L.R. Faulkner (Eds.), Electrochemical Methods: Fundamentals and Applications, Wiley, New York, 2001.
[26] S.H. Kim, J.B. Choi, Q.N. Nguyen, J.M. Lee, S. Park, T.D. Chung, J.Y. Byun, Phys. Chem. Chem. Phys. 15 (2013) 5782.
[27] S.J. Lee, Y.J. Lee, J.Y. Park, IEEE Sens. 3–6 (2013) (Nov).
[28] Deepshikha, T. Basu, Anal. Lett. 44 (2011) 1126.
[29] Y.J. Lee, D.J. Park, J.Y. Park, IEEE Sens. J. 11 (2008) 1922.
[30] Y.B. Vasil'ev, O.A. Khazova, N.N. Nikolaeva, J. Electroanal. Chem. Interfacial Electrochem. 196 (1985) 127.
[31] G.C. Bond, Molecules 17 (2012) 1716.
[32] K. Dawson, M. Baudequin, A. O'Riordan, Analyst 136 (2011) 4507.
[33] S.B. Aoun, Z. Dursun, T. Koga, G.S. Bang, T. Sotomura, I. Taniguchi, J. Electroanal. Chem. 567 (2004) 175.
[34] F. Kurniawan, V. Tsakova, V.M. Mirsky, Electroanalysis 18 (2006) 1937.
[35] G.X. Tong, F.T. Liu, W.H. Wu, J.P. Shen, X. Hua, Y. Liang, Cryst. Eng. Commun. 14 (2012) 5963.
[36] X. Niu, M. Lan, H. Zhao, C. Chen, Anal. Chem. 85 (2013) 3561.
[37] Y. Zhanga, L. Sub, D. Manuzzib, H.V.E. Monterosb, W. Jia, D. Huoa, C. Houa, Y. Lei, Biosens. Bioelectron. 31 (2012) 426.
[38] R.L. McCreery, Interfacial Electrochemistry: Theory: Experiment, and Applications, 35 (1999) 631.
[39] S. Ranganathan, T.C. Kuo, R.L. McCreery, Interfacial Electrochemistry: Theory: Experiment, and Applications, 71 (1999) 3574.
[40] B.J. Sanghavi, A.K. Srivastava, Electrochim. Acta 56 (2011) 4188.
[41] Q. Lu, S. Hu, D. Pang, Z. He, Bioelectrochemistry 86 (2012) 60.
[42] X. Niu, Y. Li, J. Tang, Y. Hu, H. Zhao, M. Lan, Biosens. Bioelectron. 51 (2014) 22.
[43] H. Bai, M. Han, Y. Du, J. Bao, Z. Dai, Chem. Commun. 46 (2010) 1739.
[44] Y. Xianyu, J. Sun, Y. Li, Y. Tian, Z. Wang, X. Jiang, Nanoscale 5 (2013) 6303.
[45] F. Cao, J. Gong, Anal. Chim. Acta. 723 (2012) 39.
[46] G. Liu, B. Zheng, Y. Jiang, Y. Cai, J. Dua, H. Yuan, D. Xiao, Talanta 101 (2012) 24.
[47] F. Huang, Y. Zhong, J. Chen, S. Li, Y. Li, F. Wang, S. Feng, Anal. Methods 5 (2013) 3050.
[48] Z.H. Ibupoto, K. Khun, V. Beni, X. Liu, M. Willander, Sensors 13 (2013) 7926.
[49] E. Reitz, W. Jia, M. Gentile, Y. Wang, Y. Lei, Electroanalysis 22 (2008) 2482.
[50] S. Sun, X. Zhang, Y. Sun, S. Yang, X. Song, Z. Yang, Chem. Phys. 15 (2013) 10904.
[51] S. Sun, X. Zhang, Y. Sun, S. Yang, X. Song, Z. Yang, ACS Appl. Mater. Interfaces 5 (2013) 4429.
[52] S.K. Meher, G.R. Rao, Nanoscale 5 (2013) 2089.
[53] J. Lin, F. Tao, L. Wang, J. Mater. Sci. 48 (2013) 5509.
[54] J. Liu, D. Xue, J. Mater. Chem. 21 (2011) 223.
[55] C. Guo, Y. Wang, Y. Zhao, C. Xu, Anal. Methods 5 (2013) 1644.
[56] F. Cao, S. Guo, H. Ma, D. Shan, S. Yang, J. Gong, Biosens. Bioelectron. 26 (2011) 2756.
[57] X. Cao, N. Wang, Electrochem. Commun. 12 (2010) 1581.
[58] X. Cao, N. Wang, Analyst 136 (2011) 4241.
[59] C.W. Kung, C.Y. Lin, Y.H. Lai, R. Vittal, K.C. Hoa, Biosens. Bioelectron. 27 (2011) 125.
[60] C. Hou, Q. Xu, L. Yin, X. Hu, Analyst 137 (2012) 5803.
[61] A.S. Kumar, P.Y. Chen, S.H. Chien, J.M. Zen, Electroanalysis 3 (2005) 17.
[62] H.B. Noh, K.S. Lee, P. Chandra, M.S. Won, Y.B. Shim, Electrochim. Acta 61 (2012) 36.
[63] Y. Miao, J. Wu, S. Zhou, Z. Yang, R. Ouyang, J. Electrochem. Soc. 160 (2013) 47.
[64] C. Li, H. Wang, Y. Yamauchi, Chem. Eur. J. 19 (2013) 2242.
[65] X. Cao, N. Wang, S. Jia, Y. Shao, Anal. Chem. 85 (2013) 5040.
[66] J.H. Shim, A. Cha, Y. Lee, C. Lee, Electroanalysis 23 (2011) 2057.
[67] M. Shao, X. Xu, J. Han, J. Zhao, W. Shi, X. Kong, M. Wei, D.G. Evans, X. Duan, Langmuir 27 (2011) 8233.
[68] Y.B. Hahn, R. Ahmadw, N. Tripathyw, Chem. Commun. 48 (2012) 10369.
[69] X. Zhang, A. Gu, G. Wang, Y. Wei, W. Wang, H. Wu, B. Fang, Cryst. Eng. Commun. 12 (2010) 1120.
[70] A.J. Wang, J.J. Feng, Z.H. Li, Q.C. Liao, Z.Z. Wang, J.R. Chen, Cryst. Eng. Commun. 14 (2012) 1289.
[71] X. Zhang, A. Gu, G. Wang, Y. Huang, H. Jia, B. Fang, Analyst 136 (2011) 5175.
[72] B. Fang, A. Gu, G. Wang, W. Wang, Y. Feng, C. Zhang, X. Zhang, ACS Appl. Mater. Interfaces 1 (2009) 2829.
[73] R. Ahmad, M. Vaseem, N. Tripathy, Y.B. Hahn, Anal. Chem. 85 (2013) 10448.
[74] S. Yu, X. Peng, G. Cao, M. Zhou, L. Qiao, J. Yao, H. He, Electrochim. Acta 76 (2012) 512.
[75] F. Cao, S. Guo, H. Ma, G. Yang, S. Yang, J. Gong, Talanta 86 (2011) 214.
[76] R. Ding, J. Liu, J. Jiang, J. Zhu, X. Huang, Anal. Methods 4 (2012) 4003.
[77] S. Luo, F. Su, C. Liu, J. Li, R. Liu, Y. Xiao, Y. Li, X. Liu, Q. Cai, Talanta 86 (2011) 157.
[78] P.V. Suneesh, K. Chandhini, T. Ramachandran, B.G. Nair, T.G.S. Babu, Biosens. Bioelectron. 50 (2013) 472.
[79] K.K. Lee, P.Y. Loh, C.H. Sow, W.S. Chin, Electrochem. Commun. 20 (2012) 128.
[80] L. Qian, J. Mao, X. Tiana, H. Yuan, D. Xiao, Sensors Actuators 176 (2013) 952.
[81] X. Zhang, L. Wang, R. Ji, L. Yu, G. Wang, Electrochem. Commun. 24 (2012) 53.
[82] Y. Wang, H. Zhong, X. Li, F. Jia, Y. Shi, W. Zhang, Z. Cheng, L. Zhang, J. Wang, Biosens. Bioelectron. 48 (2013) 56.
[83] U. Yogeswaran, S.M. Chen, Anal. Lett. 41 (2008) 210.
[84] M. Ates, Mater. Sci. Eng. C 33 (2013) 1853.
[85] A. Pandya, P.G. Sutariya, S.K. Menon, Analyst 138 (2013) 2483.
[86] H. Çiftçi, U. Tamer, React. Funct. Polym. 72 (2012) 127.
[87] F. Meng, W. Shi, Y. Sun, X. Zhu, G. Wua, C. Ruan, X. Liu, D. Ge, Biosens. Bioelectron. 42 (2013) 141.
[88] J. Shi, P. Ci, F. Wang, H. Peng, P. Yang, L. Wang, S. Ge, Q. Wang, P.K. Chu, Biosens. Bioelectron. 26 (2011) 2576.
[89] N. Cele, S.S. Ray, Macromol. Mater. Eng. 294 (2009) 719.
[90] Z. Chen, Z. Pourabedi, D.B. Hibbert, Electroanalysis 13 (1999) 11.
[91] B.J. Plowman, S.K. Bhargava, A.P. O'Mullane, Analyst 136 (2011) 5107.
[92] H. Liy, I. Deng, Anal. Chim. Acta. 300 (1995) 65.
[93] E. Lahiff, C. Lynam, N. Gilmartin, R. O'Kennedy, D. Diamond, Anal. Bioanal. Chem. 398 (2010) 1575.
[94] D.R. Kauffmanab, A. Star, Analyst 135 (2010) 2790.
[95] N.Q. Dung, D. Patil, H. Jung, D. Kim, Biosens. Bioelectron. 42 (2013) 280.
[96] L.C. Jiang, W.D. Zhang, Biosens. Bioelectron. 25 (2010) 1402.
[97] Z. Yang, J. Feng, J. Qiao, Y. Yan, Q. Yu, K. Sun, Anal. Methods 4 (2012) 1924.
[98] J. Chen, W.D. Zhang, J.S. Ye, Electrochem. Commun. 10 (2008) 1268.
[99] F. Xiao, F. Zhao, D. Mei, Z. Mo, B. Zeng, Biosens. Bioelectron. 24 (2009) 3481.
[100] D. Liu, Q. Luo, F. Zhou, Synth. Met. 160 (2010) 1745.
[101] J. Zhao, L. Wei, C. Peng, Y. Su, Z. Yang, L. Zhang, H. Wei, Y. Zhang, Biosens. Bioelectron. 47 (2013) 86.
[102] Y. Jiang, S. Yu, J. Li, L. Jia, C. Wang, Carbon 63 (2013) 367.
[103] G. Wei, F. Xu, Z. Li, K.D. Jandt, J. Phys. Chem. 115 (2011) 11453.
[104] M.B. Lerner, N. Kybert, R. Mendoza, R. Villechenon, M.A.B. Lopez, A.T.C. Johnson, Appl. Phys. Lett. 102 (2013) 183113.
[105] Bo He, Liji Hong, Juan Lu, Jianguo Hu, Yunyun Yang, Junhua Yuan, Li Niu, Electrochim. Acta 91 (2013) 353.

[106] S. Wu, Q. He, C. Tan, Y. Wang, H. Zhang, Small 8 (2013) 1160.
[107] M. Liu, R. Liu, W. Chen, Biosens. Bioelectron. 45 (2013) 206.
[108] W. Lv, F.M. Jin, Q. Guo, Q.H. Yang, F. Kang, Electrochim. Acta 73 (2012) 129.
[109] G. Wu, X. Song, Y. Wu, X. Chen, F. Luo, X. Chen, Talanta 105 (2013) 379.
[110] H. Gao, F. Xiao, C.B. Ching, H. Duan, ACS Appl. Mater. Interfaces 3 (2011) 3049.
[111] X. Wang, X. Dong, Y. Wen, C. Li, Q. Xiong, P. Chen, Chem. Commun. 48 (2012) 6490.
[112] F. Xiao, Y. Li, H. Gao, S. Ge, H. Duan, Biosens. Bioelectron. 41 (2013) 417.
[113] F.Y. Kong, X.R. Li, W.W. Zhao, J.J. Xu, H.Y. Chen, Electrochem. Commun. 14 (2012) 59.
[114] J.C. Ndamanisha, L. Guo, Anal. Chim. Acta. 747 (2012) 19.
[115] L. Luo, F. Li, L. Zhu, Y. Ding, Z. Zhang, D. Deng, B. Lu, Colloids Surf. B 102 (2013) 307.
[116] D. Gu, H. Bongard, Y. Deng, D. Feng, Z. Wu, Y. Fang, J. Mao, B. Tu, F. Schüth, D. Zhao, Adv. Mater. 22 (2010) 833.
[117] X. Bo, J. Bai, L. Yang, L. Guo, Sensors Actuators 157 (2011) 662.
[118] K.M.E. Khatiba, R.M.A. Hameedb, Biosens. Bioelectron. 26 (2011) 3542.
[119] R.M.A. Hameed, Biosens. Bioelectron. 47 (2013) 248.
[120] A. Liu, Q. Ren, T. Xu, M. Yuan, W. Tang, Sensors Actuators 162 (2012) 135.
[121] J.H.T. Luong, K.B. Male, J.D. Glennon, Analyst 134 (2009) 1965.
[122] H. Sim, J.H. Kim, S.K. Lee, M.J. Song, D.H. Yoon, D.S. Lim, S.I. Hong, Thin Solid Films 520 (2012) 7219.
[123] C.Y. Ko, J.H. Huang, S. Raina, W.P. Kang, Analyst 138 (2013) 3201.
[124] Y. Zhao, Z. He, Z. Yan, Analyst 138 (2013) 559.
[125] D. Ye, G. Liang, H. Li, J. Luo, S. Zhang, H. Chen, J. Kong, Talanta 116 (2013) 223.

Kun Tian is currently pursuing her Ph.D. degree in the Department of Materials Science and Engineering at the University of Utah. She obtained a B.E. degree in Materials Science and Engineering from the Shenyang Jianzhu University, Shenyang, China, in 2013. Her current research interests are in the field of developing nanostructured materials for biological, environmental, and energy applications.

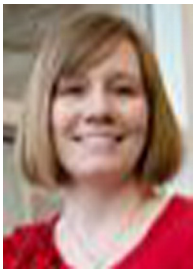

Megan Campbell Prestgard is currently pursuing her Ph.D. in Materials Science and Engineering at the University of Utah. She obtained a B.S. in Materials Science and Engineering from the University of Utah in 2012. Her current research interests include the fabrication, characterization, and modification of materials for application in spintronic devices.

Ashutosh Tiwari is an Associate Professor and the Director of Nanostructured Materials Laboratory at the University of Utah. He obtained his M.S. in physics in 1993 from the Indian Institute of Technology Delhi and Ph.D. in Physics in 2000 from the Indian Institute of Technology Kanpur. After doing postdocs at the University of Delaware (1999–2001) and the North Carolina State University (2001–2005), he joined the University of Utah in the year 2005 as an assistant professor. He was promoted to the rank of a tenured associate professor in 2010. He has published extensively on the various aspects of nanotechnology and materials science. He has received several prestigious awards including the U. S. National Science Foundation's CAREER Award.